Changes in the Chondrocyte and Extracellular Matrix Proteome during Post-natal Mouse Cartilage Development*[S]

Richard Wilson‡§¶, Emma L. Norris‖, Bent Brachvogel‡‡, Constanza Angelucci‡, Snezana Zivkovic‡, Lavinia Gordon‡, Bianca C. Bernardo‡§§, Jacek Stermann‡‡, Kiyotoshi Sekiguchi¶¶, Jeffrey J. Gorman‖, and John F. Bateman‡‖‖***

Skeletal growth by endochondral ossification involves tightly coordinated chondrocyte differentiation that creates reserve, proliferating, prehypertrophic, and hypertrophic cartilage zones in the growth plate. Many human skeletal disorders result from mutations in cartilage extracellular matrix (ECM) components that compromise both ECM architecture and chondrocyte function. Understanding normal cartilage development, composition, and structure is therefore vital to unravel these disease mechanisms. To study this intricate process *in vivo* by proteomics, we analyzed mouse femoral head cartilage at developmental stages enriched in either immature chondrocytes or maturing/hypertrophic chondrocytes (postnatal days 3 and 21, respectively). Using LTQ-Orbitrap tandem mass spectrometry, we identified 703 cartilage proteins. Differentially abundant proteins ($q < 0.01$) included prototypic markers for both early and late chondrocyte differentiation (epiphycan and collagen X, respectively) and novel ECM and cell adhesion proteins with no previously described roles in cartilage development (tenascin X, vitrin, Urb, emilin-1, and the sushi repeat-containing proteins SRPX and SRPX2). Meta-analysis of cartilage development *in vivo* and an *in vitro* chondrocyte culture model (Wilson, R., Diseberg, A. F., Gordon, L., Zivkovic, S., Tatarczuch, L., Mackie, E. J., Gorman, J. J., and Bateman, J. F. (2010) Comprehensive profiling of cartilage extracellular matrix formation and maturation using sequential extraction and label-free quantitative proteomics. *Mol. Cell. Proteomics* 9, 1296–1313) identified components involved in both systems, such as Urb, and components with specific roles *in vivo*, including vitrin and CILP-2 (cartilage intermediate layer protein-2). Immunolocalization of Urb, vitrin, and CILP-2 indicated specific roles at different maturation stages. In addition to ECM-related changes, we provide the first biochemical evidence of changing endoplasmic reticulum function during cartilage development. Although the multifunctional chaperone BiP was not differentially expressed, enzymes and chaperones required specifically for collagen biosynthesis, such as the prolyl 3-hydroxylase 1, cartilage-associated protein, and peptidyl prolyl *cis-trans* isomerase B complex, were down-regulated during maturation. Conversely, the lumenal proteins calumenin, reticulocalbin-1, and reticulocalbin-2 were significantly increased, signifying a shift toward calcium binding functions. This first proteomic analysis of cartilage development *in vivo* reveals the breadth of protein expression changes during chondrocyte maturation and ECM remodeling in the mouse femoral head. *Molecular & Cellular Proteomics 11: 10.1074/mcp.M111.014159, 1–18, 2012.*

Cartilage is a unique tissue characterized by an abundant extracellular matrix (ECM)[1] and a single cell type, the chondrocyte. However, the permanent hyaline cartilage, which provides the articulating surfaces of long bones and vertebrae, and the transient growth plate cartilage responsible for endochondral bone growth are uniform in neither cellular phenotype nor protein composition. In articular cartilage, the chondrocytes form morphologically distinct regions comprising a superficial region of flattened cells, a sparsely populated middle layer, and a deep zone of hypertrophic chondrocytes embedded in calcified cartilage at the chondro-osseous junc-

From the ‡Murdoch Childrens Research Institute, Royal Children's Hospital, Parkville, Melbourne, Victoria 3052, Australia, the §Central Science Laboratory, University of Tasmania, Hobart, Tasmania 7001, Australia, the ‖Protein Discovery Center, Queensland Institute of Medical Research, Royal Brisbane Hospital, Herston, Queensland 4029, Australia, the **Center for Molecular Medicine Cologne, University of Cologne, 50931 Cologne, Germany, the ‡‡Medical Faculty, Center for Biochemistry, University of Cologne, 50931 Cologne, Germany, the ¶¶Institute for Protein Research, Osaka University, Suita, Osaka 565-0871, Japan, the ‖‖Department of Biochemistry and Molecular Biology, University of Melbourne, Parkville, Victoria 3052, Australia, and the §§Department of Pediatrics, University of Melbourne, Parkville, Victoria 3052, Australia

Received September 5, 2011, and in revised form, October 10, 2011

Published, MCP Papers in Press, October 11, 2011, DOI 10.1074/mcp.M111.014159

[1] The abbreviations used are: ECM, extracellular matrix; LTQ, linear trap quadrupole; FDR, false discovery rate; GdnHCl, guanidinium hydrochloride; DAVID, Database for Annotation, Visualization and Integrated Discovery; GO, gene ontological; P*n*, post-natal day *n*; ER, endoplasmic reticulum; COMP, cartilage oligomeric matrix protein; TGF, transforming growth factor.

tion. In mature articular cartilage, these chondrocytes divide infrequently. In contrast, the active division and expansion of chondrocytes in growth plate cartilage is the primary mechanism for growth of the axial and appendicular skeletal elements (see Fig. 1). Growth plate chondrocytes enter the maturation process from a pool of reserve zone cells in the epiphyseal cartilage most distal to the chondro-osseous junction. These small round cells differentiate into discoid proliferating chondrocytes that align into columns and dictate the axis of bone growth. The chondrocytes then enter a postmitotic prehypertrophic phase and expand in volume to form fully differentiated hypertrophic chondrocytes that provide a niche for vascular invasion and remodeling of the cartilage into bone (1).

In humans, disruption of chondrocyte maturation in the growth plate results in inherited skeletal dysplasias ranging in severity from mild dwarfism (*e.g.* metaphyseal chondrodysplasia, Schmid type) and early onset osteoarthritis (*e.g.* multiple epiphyseal dysplasia) to perinatal lethality (*e.g.* achondrogenesis). Although individually rare, these skeletal dysplasias collectively affect 2–5 per 10,000 live born (reviewed in Ref. 2). Mutations underlying skeletal dysplasias frequently compromise the precise assembly and interaction of cartilage ECM components, highlighting the critical role of ECM networks in chondrocyte differentiation, organization, and survival (3). In addition to a loss of ECM integrity, endoplasmic reticulum (ER) stress and activation of the unfolded protein response contribute to the pathology (4).

Microarray analysis of microdissected mouse cartilage zones has generated differential mRNA expression profiles of chondrocyte subpopulations (5–7). However, proteomics level analysis of cartilage development is challenging because of the limited available tissue and dominance of poorly soluble matrix components (8). Novel methods developed for proteomic analysis of growth plate and articular cartilage (9–11), in particular using solubility-based tissue fractionation, have improved coverage of both the intracellular and extracellular cartilage proteome using both two-dimensional electrophoresis and capillary HPLC-tandem MS (12, 13). In this study we used mouse femoral head cartilage to identify novel proteins associated with chondrocyte differentiation and cartilage development *in vivo*. Developmental stages with clear differences in chondrocyte differentiation states were selected based on histomorphology and FACS. At post-natal day 3 (P3), femoral head cartilage is populated predominantly by immature reserve chondrocytes, which at 3 weeks (P21) are largely replaced by maturing prehypertrophic and hypertrophic cells.

Proteomic analysis of P3 and P21 cartilage extracts using label-free quantitative mass spectrometry identified 703 nonredundant proteins with high confidence. Using the beta-binomial distribution to model the spectral count data, we identified 146 significant differentially expressed proteins ($q < 0.01$). To extract functional information from the group of differentially expressed proteins, enriched gene ontological (GO) terms were identified using the Database for Annotation, Visualization and Integrated Discovery (DAVID). Many of the differentially expressed proteins were novel in the context of cartilage development, including ECM components, cell adhesion proteins, and a group of calcium-binding ER lumenal proteins, the reticulocalbins. The results of our proteomic analysis were validated by immunohistochemistry analysis of selected ECM components, revealing distinct regional expression patterns associated with zones of chondrocyte proliferation, maturation, and hypertrophy.

EXPERIMENTAL PROCEDURES

Cartilage Dissection and Chondrocyte Preparation for Fluorescence-activated Cell Sorting—Femoral head cartilage was obtained from 3- and 21-day post-natal C57/Bl6 mice by dislocation of the hip joint, fracture at the femoral neck, and removal of the *ligamentum teres* at the insertion site. The dissected cartilage was rinsed in PBS, frozen on dry ice, and stored at −80 °C in batches of eight P3 hips and six P21 hips, equivalent to ~10 mg of wet weight of tissue. Dissected femoral heads from P3 and P21 mice were also used to characterize the distribution of novel cartilage proteins by immunohistochemistry.

To analyze P3 and P21 chondrocytes by FACS, femoral heads were incubated for 2 h at 37 °C in DMEM containing 5% FCS and 2 mg/ml bacterial collagenase (Worthington Biochemicals). Chondrocytes were resuspended in PBS containing 5% FCS (6×10^3 cells/ml in 50 ml) and incubated with primary conjugated antibodies specific for CD24a and CD200 (Becton Dickinson) for 15 min on ice. The cells were subsequently washed and co-stained with 7-aminoactinomycin D for dead cell detection, followed by flow cytometry (FACSCantoII). The corresponding IgG isotypes (Becton Dickinson) were used as negative controls.

Protein Extraction—The P3 and P21 femoral head cartilage (three independent batches of tissue per developmental stage) was pulverized using a liquid nitrogen-cooled tissue grinder and transferred to Eppendorf tubes. Sequential protein extracts were prepared using a nondenaturing buffer (1 M NaCl in 100 mM Tris acetate, pH 8.0) followed by a chaotropic buffer (4 M GdnHCl, 65 mM DTT, 10 mM EDTA in 50 mM sodium acetate, pH 5.8) as described (13). The guanidine-extracted proteins were further partitioned by molecular mass cut-off filtration through a 100-kDa cut-off ultracentrifugal column (Amicon). Protein extracts were precipitated with 9 volumes of ethanol, and protein pellets washed twice in 70% (v/v) ethanol and resuspended in 150 μl of solubilization buffer containing 7 M urea, 2 M thiourea, 4% CHAPS, and 30 mM Tris, pH 8.0. Protein concentrations were estimated using the Bradford assay (Pierce).

SDS-PAGE and Immunoblotting—Cartilage extracts were analyzed by SDS-PAGE to assess reproducibility and relative levels of cartilage proteins in each of the femoral head cartilage fractions. Aliquots of each extract equivalent to 2% of the total protein yield were heated in Laemmli buffer containing 50 mM dithiothreitol for 15 min at 65 °C and resolved through 4–12% acrylamide Bis-Tris NuPAGE gels (Invitrogen), and proteins were visualized by silver staining as described (14).

Protein Reduction, Alkylation, and In-solution Trypsin Digestion—Protein samples for LC-MS/MS analysis were sequentially reduced and alkylated under nitrogen by incubation in 10 mM dithiothreitol (overnight at 4 °C) and then 50 mM iodoacetamide (2 h at 25 °C in the dark). Proteins were co-precipitated with 1 μg of trypsin (Promega) overnight at −20 °C in 1 ml of methanol. The trypsin-protein precipitates were washed once with chilled methanol, dried, and reconstituted in 100 mM ammonium bicarbonate, followed by trypsinization at

37 °C for 5 h, with the addition of 1 μg of trypsin after 2 h. Digests were terminated by freezing on dry ice.

Orbitrap Mass Spectrometry—Each of the three fractions per sample was analyzed in duplicate by LC-MS/MS using an UltiMate 3000 HPLC system (Dionex) or a Tempo NanoLC system (Eksigent) in line with an LTQ-Orbitrap XL (ThermoFisher Scientific). Aliquots of tryptic peptides equivalent to 25% of the in-solution digests were loaded onto a 0.3 × 5-mm C_{18} trap column (Dionex) at 20 μl/min in 98% solvent A (0.1% (v/v) formic acid) and 2% solvent B (80% (v/v) acetonitrile, 0.1% (v/v) formic acid) for 5 min and subsequently backflushed onto a pre-equilibrated analytical column (Vydac Everest C_{18} 300 Å, 150 μm × 150 mm; Alltech) using a flow rate of 1 μl/min. Peptides were separated at 40 °C using three linear gradient segments (2–12% solvent B over 6 min, 12–50% solvent B over 65 min, and then 50–100% solvent B over 15 min), holding at 100% solvent B for a further 15 min before returning to 2% solvent B over 5 min.

The LTQ-Orbitrap was fitted with a dynamic nanoelectrospray ion source (Proxeon) containing a 30-μm inner diameter uncoated silica emitter (New Objective). The LTQ-Orbitrap XL was controlled using Xcalibur 2.0 software (Thermo Electron) and operated in data-dependent acquisition mode whereby the survey scan was acquired in the Orbitrap with a resolving power set to 60,000 (at 400 *m/z*). MS/MS spectra were concurrently acquired in the LTQ mass analyzer on the seven most intense ions from the FT survey scan. Charge state filtering, where unassigned precursor ions were not selected for fragmentation, and dynamic exclusion (repeat count, 1; repeat duration, 30 s; exclusion list size, 500) were used. Fragmentation conditions in the LTQ were: 35% normalized collision energy, activation *q* of 0.25, 50-ms activation time, and minimum ion selection intensity of 500 counts.

Database Searching—The acquired MS/MS data, together with MS/MS data acquired in our previous LC-MS/MS cartilage proteomics study (12), were analyzed using Mascot version 2.2.06 (Matrix Science). Proteome Discoverer version 1.2 (Thermo Scientific) was used to extract tandem mass spectra from Xcalibur raw files and submit searches to an in-house Mascot server according to the following parameters: *S*-carboxamidomethylation of cysteine residues specified as a fixed modification and cyclization of N-terminal glutamine to pyroglutamic acid, deamidation of asparagine, hydroxylation of proline, oxidation of methionine specified as variable modifications. Parent ion tolerance of 20 ppm and fragment ion mass tolerances of 0.8 Da were used, and enzyme cleavage was set to trypsin, allowing for a maximum of two missed cleavages. The database searched consisted of 46,137 sequences, comprising the UniProt complete proteome set for *Mus musculus* (45,889 sequences downloaded on May 23, 2011) and sequences for common contaminants appended (downloaded from the Max Plank Institute http://maxquant.org). The automatic Mascot decoy database search was performed for all data sets.

Criteria for Protein Identification—The Mascot search results were loaded into Scaffold version 3.0.08 to assign probabilities to peptide and protein matches (15). Peptide-spectrum matches were accepted if the peptide was assigned a probability greater than 0.95 as specified by the Peptide Prophet algorithm (16). The probability threshold of 0.95 showed good discrimination between the predicted correct and incorrect peptide-spectrum assignments, and only peptides with charge states of +1, +2, and +3 were retained as confident identifications because the Peptide Prophet models were not a good fit to the data for charge states ≥4. Protein identifications were accepted if the protein contained at least two unique peptides (in terms of amino acid sequence), and the protein was assigned a probability >0.99 by the Protein Prophet algorithm (17). This threshold will constrain the protein false discovery rate (FDR) to <1%. The minimal list of proteins that satisfy the principal of parsimony is reported.

Statistical and Bioinformatic Analysis of Tandem Mass Spectrometry Data—To obtain sample level spectral count data, MS/MS data for the E0, E1, and E2 fractions for each replicate sample were recombined *in silico* using the Scaffold MudPIT function. Global normalization was applied to the raw spectral counts, and a pseudo count of one was added to reduce the effect of undersampling. Fold changes were estimated using the mean of the normalized counts for P21 relative to P3. The beta-binomial test (18) was used to assess the differences between the P3 and P21 samples. This test models the magnitude of the differences in spectral counts between the sample groups and the variation between replicate measurements. QVALITY was applied to estimate *q* values for each protein (19), where a *q* value is the minimum FDR at which the protein can be called significant. A *q* value of 0.01 was used as the significance threshold in this study.

Functional annotation and enrichment analysis was performed using the DAVID version 6.7 (20). Protein lists were uploaded as the official gene symbols to the DAVID website (http://david.abcc.ncifcrf.gov/) using the complete mouse genome as background. Significantly enriched functional groups were ranked using the functional annotation clustering tool set to the high classification stringency.

Immunohistochemical Analysis—Femoral heads isolated from P3 and P21 C57/Bl6 mice were fixed with 4% (v/v) paraformaldehyde in PBS overnight at 4 °C, followed by incubation in decalcification solution (Immunocal) for 18 h at 4 °C. Tissues were washed in PBS and processed (Leica TP 1010 automated tissue processor) prior to embedding in liquid paraffin wax. Saggittal sections of femoral heads (5 μm) were cut using a Leica 1512 microtome and then baked at 60 °C for 1 h. Three-week neocartilage culture (*in vitro* chondrocyte culture day 21) specimens were processed as described (12). Paraffin sections were dewaxed in xylene and bought to water with graded ethanol, followed by two rinses in tap water and two rinses in PBS.

Two methods were used for antigen retrieval. For Urb and vitrin analysis, slides were incubated in 2 mg/ml pepsin for 30 min at 37 °C followed by 10 mM citrate buffer containing 0.05% Tween 20 at 60 °C for 30 min. The cooled slides were washed in PBS and then treated with 0.2% hyaluronidase (Type IV-S) for 60 min at 37 °C, followed by three PBS washes. For the CILP-2 analysis, the slides were heat treated with 10 mM Tris, 1 mM EDTA, pH 8, at 60 °C for 30 min. The cooled slides were treated with 30 μg/ml proteinase K in 50 mM Tris, pH 6.0, 5 mM $CaCl_2$ for 30 min at 37 °C and then 0.2% hyaluronidase (Type IV-S) for 60 min at 37 °C. Endogenous peroxidases were inactivated for 30 min using 3% H_2O_2 (v/v) in PBS.

Tissue sections were blocked with goat serum (Vectastain Elite ABC rabbit IgG kit) in 1% BSA in PBS for 60 min prior to overnight incubation with rabbit polyclonal antibodies to vitrin (2 μg/ml), Urb (0.2 μg/ml) (21), or CILP-2 (22) (2 μg/ml). Control sections were probed with the preimmune serum (CILP-2) or nonimmune rabbit IgGs (Urb and vitrin) at the same concentration as the primary antibodies. Biotinylated secondary antibody (Vectastain Elite ABC rabbit IgG kit) was applied to sections for 1 h, and sections washed in three changes of PBS and then incubated with ABC reagent (Vectastain Elite ABC rabbit IgG kit) for 30 min at room temperature. The sections were washed again in PBS, with immunohistochemical staining detected using ImmPact DAB substrate (Vector Laboratories) until color was detected. The reactions were terminated by rinsing in tap water, followed by dehydration of tissue sections using a graded ethanol series (50, 70, 90, and 100%). The images were captured at 10× magnification with a Nikon Eclipse 80i microscope.

RESULTS

Femoral Head Cartilage as a Model for Mouse Cartilage Development in Vivo—Endochondral ossification, the process

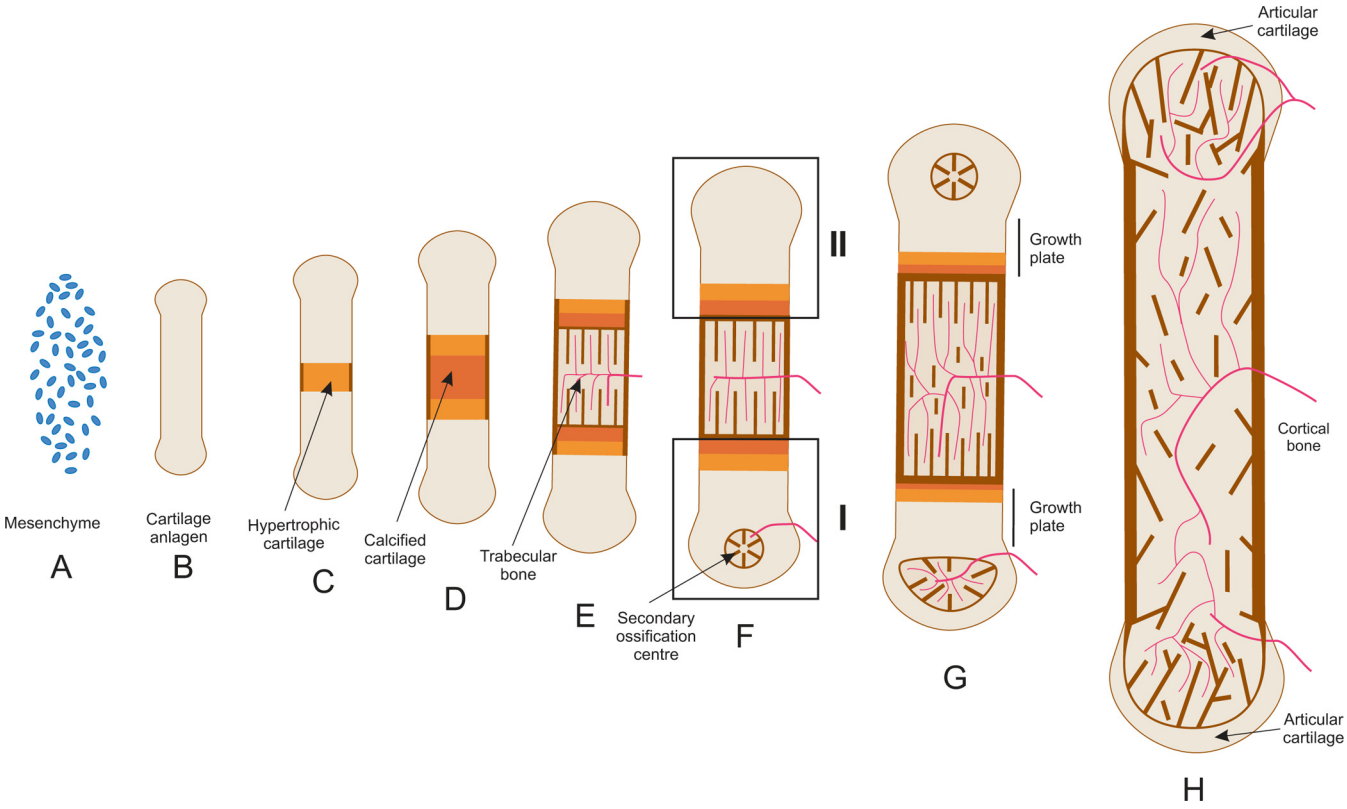

FIG. 1. **The role of cartilage in endochondral ossification.** *A* and *B*, mesenchymal cells condense and differentiate to form chondrocytes that synthesize a collagen II and aggrecan-rich ECM, providing a cartilage template (analage) for endochondral ossification. *C*, the primary ossification process is initiated as chondrocytes in the center undergo maturation to hypertrophy. *D* and *E*, the hypertrophic cartilage is calcified and provides the niche for vascular invasion. The calcified cartilage is replaced by primary bone that is subsequently remodeled to form secondary bone and bone marrow. This process radiates outwards from the center of the anlage with development of highly ordered growth plates that separate the cartilaginous epiphysis from the bony diaphysis. *F* and *G*, as the bone grows, secondary ossification centers are formed within the epiphyses by chondrocytes, which stop proliferating and undergo hypertrophy. This occurs at different rates in different epiphyses. *H*, in humans the primary and secondary ossification centers fuse after puberty, whereas in adult mice a narrow region of growth plate cartilage remains.

by which cartilaginous precursors are remodeled into bone, begins in different skeletal elements at different developmental stages. Therefore, our first aim was to establish a developmental model suitable for proteomic analysis. In the mouse femur, secondary ossification of the distal epiphyseal cartilage (corresponding to the *lower boxed region* I in Fig. 1) begins early in post-natal development (23). This limits the available cartilage to the growth plate, which can only be collected by tissue sectioning and microdissection (9). In contrast, the proximal femoral head at the hip (corresponding to the *upper boxed region* II in Fig. 1) remains devoid of trabecular bone until the onset of skeletal maturity (24) and can be dissected as an intact explant of articular cartilage and underlying primary growth plate (25).

Developmental changes in the femoral head were characterized by hematoxylin and eosin staining of saggittal sections cut through P3 and P21 cartilage explants (Fig. 2*A*). In P3 cartilage, with the exception of the proliferative chondrocytes in the growth plate, most of the cells were round and immature, with little morphological distinction between the articular cartilage surface and the presumptive ossification center. In contrast, the P21 ossification center, also described in the femoral head as the articular cartilage deep zone (26), was predominantly replaced by hypertrophic cartilage, and the articular cartilage showed evidence of differentiation into superficial and middle chondrocyte zones.

To quantify this cellular maturation process, cells released from P3 and P21 cartilage were analyzed by FACS (Fig. 2*B*). We used validated cell surface markers of defined chondrocyte differentiation states, previously identified by microarray profiling of mouse growth plate chondrocytes (27). CD24a is expressed at the surface of both immature and mature chondrocytes, and CD200 expression is restricted to the prehypertrophic and hypertrophic cells. The increased population of $CD24a^{+}/CD200^{+}$ chondrocytes in P21 cartilage (66 ± 1.2%) compared with P3 cartilage (37.3 ± 2.3%) provided further evidence of chondrocyte differentiation. On this basis, we used P3 and P21 femoral head cartilage to investigate protein expression changes during chondrocyte maturation and cartilage ECM development.

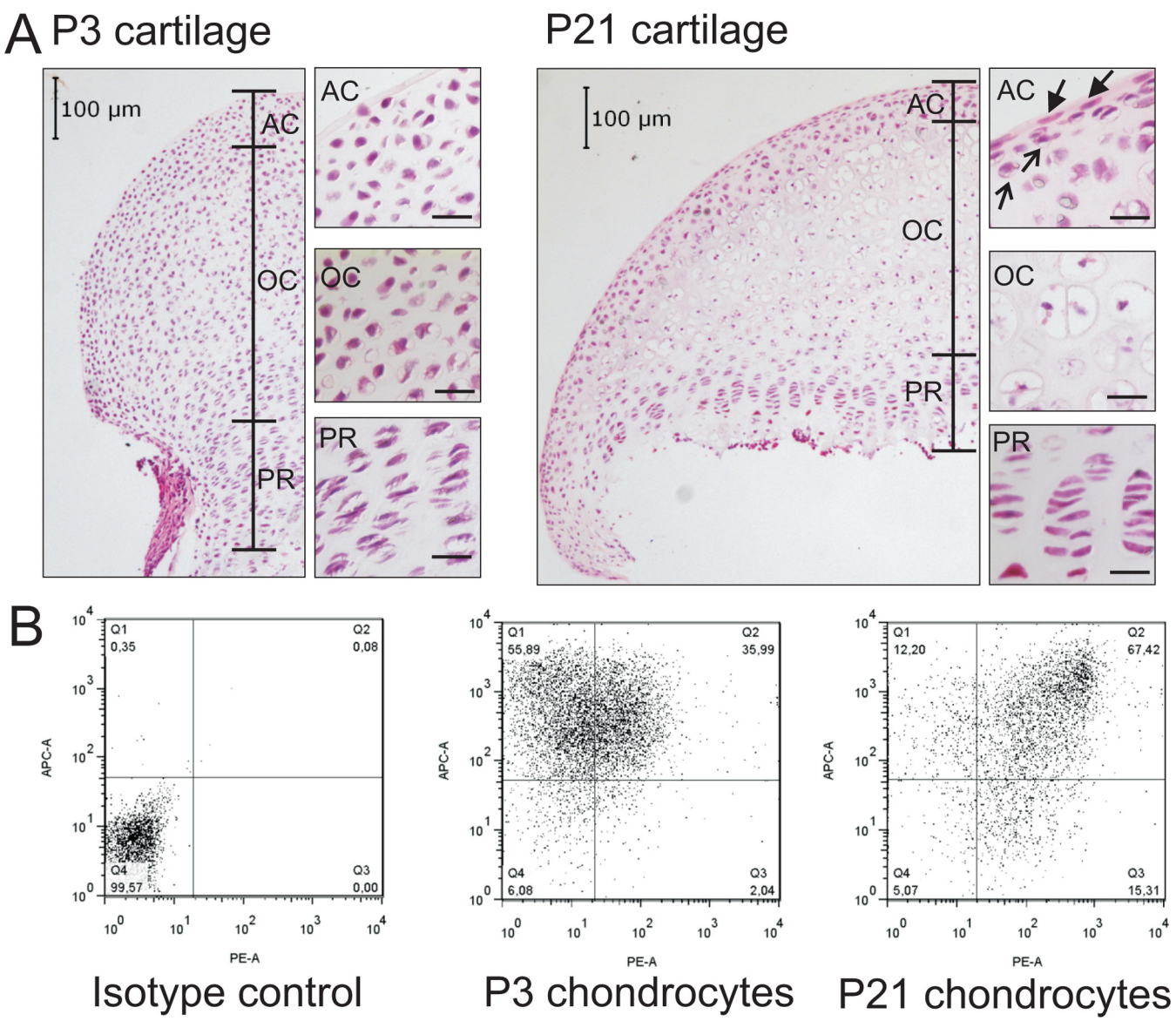

FIG. 2. **Characterization of femoral head model for cartilage development at the tissue and cellular level.** *A*, hematoxylin and eosin staining to show changes in cartilage histology between 3 days (P3) and 21 days (P21) of post-natal development. The presumptive ossification center (*OC*) of P3 cartilage, populated by immature chondrocytes, is largely replaced at P21 by hypertrophic cartilage. In P3 cartilage, the articular chondrocytes (*AC*) are homogeneous, whereas in P21 cartilage, superficial (*arrows*) and mid-zone (*filled arrows*) articular chondrocytes are more clearly distinguishable. At both stages, flattened columns of proliferative (*PR*) chondrocytes are evident in the growth plate. *B*, fluorescence-activated cell sorting of P3 and P21 chondrocytes to differentiate between chondrocyte differentiation states. Chondrocytes were prepared and sorted in three independent experiments, and representative plots are shown. All chondrocytes are labeled with antibodies to CD24a (*y axis*), whereas CD200 (*x axis*) is a marker for prehypertrophic and hypertrophic chondrocytes. The increased proportion of $CD24a^{+}/CD200^{+}$ cells (*Q2*) relative to $CD24a^{+}/CD200^{-}$ cells (*Q1*) is consistent with an increased number of mature chondrocytes.

Sequential Extraction and Analysis of Femoral Head Cartilage Protein Fractions—A significant fraction of the cartilage proteome consists of extracellular matrix that must be dissociated using a strong denaturant such as GdnHCl. We used sequential extraction based on differential solubility in 1 M NaCl and 4 M GdnHCl followed by centrifugal ultrafiltration to further separate the guanidine-soluble components (13). This method, shown schematically in Fig. 3*A*, partitions the cartilage proteome into three distinct fractions, effectively reducing sample complexity and increasing proteome coverage (12). Protein yields from P3 and P21 cartilage extracts were ~25 μg/mg of wet tissue, consistent with previous studies (10, 13).

Analysis of the P3 and P21 cartilage protein fractions by SDS-PAGE revealed consistent band profiles between replicate extractions, but marked differences were observed in the ratios of readily soluble (E0) and poorly soluble (E1 and E2) proteins between the two maturation states (Fig. 3*B*). In P3

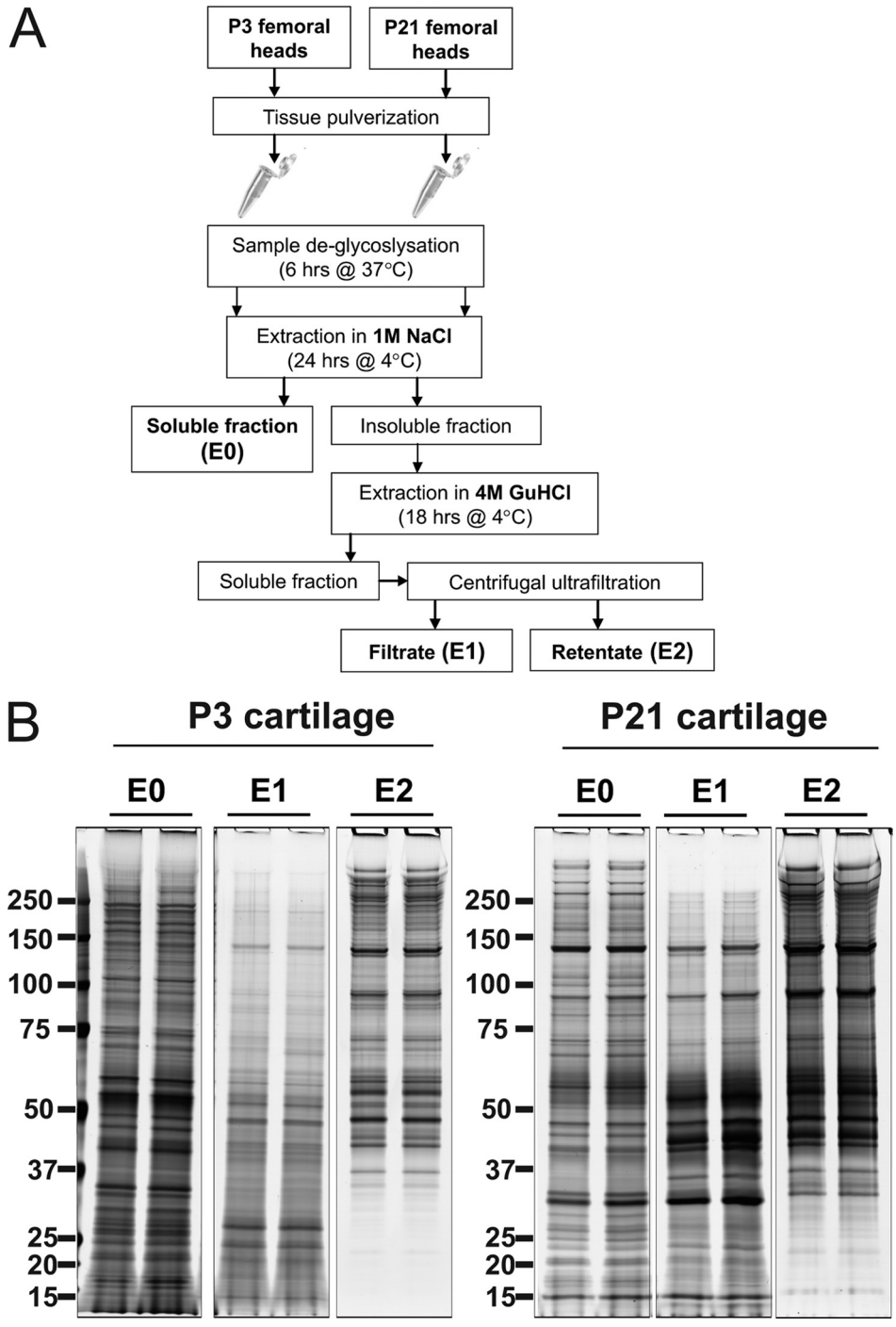

FIG. 3. **Sequential extraction of femoral head cartilage.** *A*, protein extraction from cartilage using a combination of physical (pulverization), chemical (4 M GdnHCl), and enzymatic (deglycosylation using chondroitinase ABC) methods to disrupt the extracellular matrix. The readily soluble 1 M NaCl extract (*E0*) is not fractionated further, whereas the 4 M GdnHCl extract is further separated by centrifugal ultrafiltration into nominal low (*E1*) and high (*E2*) molecular mass fractions. *B*, SDS-PAGE profiles of femoral head cartilage protein extracts to show reproducibility between biological replicates and the effective partitioning of cartilage proteins into three distinct fractions. Aliquots of replicate sequential extracts from 3-day (*P3*) and 21-day (*P21*) cartilage equivalent to 2% of the protein yield were resolved by Bis-Tris 4–12% NuPAGE, and the proteins were visualized by silver staining.

cartilage, a higher proportion of the material was soluble in 1 M NaCl, whereas in P21 cartilage, more protein was extracted in 4 M GdnHCl. This increase in the relative abundance of poorly soluble proteins is consistent with the biosynthesis and integration of increasingly insoluble networks during maturation of the cartilage extracellular matrix.

Label-free NanoLC Tandem Mass Spectrometry—P3 and P21 femoral head cartilage protein fractions were trypsin-digested in solution. The peptides were resolved by capillary HPLC and analyzed by LTQ-Orbitrap tandem MS. The MS/MS data were submitted to Mascot, and analysis of search results using Scaffold resulted in the identification of 70,318 peptide-spectrum matches with a probability greater than 0.95 (charge states $\leq$ 3). The FDR at the peptide-spectrum level was 0.56%, based on the ratio of 392 decoy matches to 69,926 target matches. The complete list of peptides identified in this study is included in supplemental Table 1. After the peptides were assembled into proteins, and the principle of parsimony was applied there were 703 proteins (and one decoy protein) identified with two or more unique peptides and a protein probability of >0.99.

The number of peptide-spectrum matches assigned to each protein was used as a measure of relative protein abundance, and global normalization was used to correct for any systematic variations. The complete set of normalized spectral counts is presented in supplemental Table 2*A*. The beta-binomial test, which estimates the likelihood that a difference of the same or greater magnitude would be observed by chance (18), was used to compare normalized counts for P3 and P21 samples. To correct for multiple comparisons, *q* values were assigned to each protein in the data set, where the *q* value is the minimum FDR at which an observation can be called significant (28). To select an appropriate significance threshold, normalized counts for P3 and P21 were represented using MA plots (29). Significant proteins are highlighted at *q* value thresholds of 0.001, 0.01, and 0.05, and the null distribution for two biological replicates are presented (Fig. 4). We chose a threshold of $q < 0.01$, at which 146 proteins were identified as differentially abundant, and less than two of these are expected false positives.

Protein Functional Categories Associated with Cartilage Development—We used the web-based resource DAVID (20) to extract biological meaning from the set of 146 differentially abundant proteins. Using a functional annotation tool set to high stringency, 20 clusters were significant with an enrichment score of >2 (shown in supplemental Table 3*A*). Annotation clusters with the greatest number of entries were the cellular components "extracellular matrix" (cluster 1; $n = 28$) and "intracellular organelle lumen" (cluster 19; $n = 22$). Of the significant ECM components, 11 were more abundant in P3 cartilage, and 17 were more abundant in P21 cartilage, signifying extensive remodeling and changes in matrix structure during cartilage maturation. The modular nature of ECM constituents allows multiple interactions and modified functionality in different tissue matrices. Accordingly, three enriched terms were protein structural domains that occur frequently in ECM components: thrombospondin, type III repeat (cluster 11; $n = 3$), EGF-like region, conserved site (cluster 9; $n = 10$), and leucine-rich repeat (cluster 18; $n = 7$) that comprised the small leucine-rich repeat proteoglycans. The critical role of cartilage proteoglycans was also highlighted by the term polysaccharide binding (cluster 2; $n = 12$), which included the major cartilage proteoglycan aggrecan (Acan), one aggrecan-binding protein (cartilage oligomeric matrix protein, COMP), and the superficial zone proteoglycan lubricin (Prg4). A further group of components involved in cell-matrix interactions, described by the term positive regulation of cell adhesion (cluster 15; $n = 5$), were all significantly increased in P21 cartilage. Thrombospondin-1 is a known chondrocyte-binding protein (30), whereas the other four cell adhesion proteins were either entirely novel cartilage constituents (tenascin X and emilin-1) or have never been described in post-natal cartilage (coiled-coil domain-containing protein 80/Urb and vitrin). The ECM and cell-matrix adhesion proteins described by these six enriched functional terms are presented in Table I.

Several annotation clusters were related to the rough ER and protein secretion, and the trends for these intracellular protein groups are represented in Fig. 5 (*A* and *B*). The enriched terms "oxoglutarate and iron-dependent oxygenase" and "procollagen-proline dioxygenase activity" (clusters 6 and 10, respectively) included prolyl 4-hydroxylase, lysyl hydroxlyase, and prolyl 3-hydroxylase enzymes ($n = 5$), which are involved in the post-translational modification of collagen α chains (31). The prolyl 4-hydroxylase β subunit (P4hb) is an ER protein disulfide isomerase and among the proteins in the enriched annotation term "protein disulfide isomerase activity" (cluster 8; $n = 4$). One further cellular protein subset related to protein biosynthesis was classified as "ribonucleoprotein" (cluster 4; $n = 12$). The final group of ER proteins were the calcium-binding lumenal proteins classified by the PIR superfamily "reticulocalbin" (cluster 14; $n = 3$). With the notable exception of the reticulocalbins, the proteins associated with these enriched annotation clusters were more abundant in P3 cartilage.

The sequential extraction method used in this study partitions cartilage proteins according to solubility, for example separating macromolecular complexes from readily soluble cytosolic enzymes (12). The ratios of E0, E1, and E2 fractions between P3 and P21 developmental stages changed significantly (Fig. 3). Therefore, we examined three differentially soluble protein subsets to verify that the described differences in protein abundance did not result from a global shift in protein extractability. Accordingly, the 14-3-3 proteins (1 M NaCl-soluble), tubulin chains, and T-complex chaperonin subunits (4 M GdnHCl-soluble) showed no evidence for differential abundance in P3 and P21 cartilage (Fig. 5*C*).

Meta-analysis of Two Cartilage Developmental Models—We recently identified a cohort of ECM components and markers for chondrocyte differentiation by comparison of mouse juvenile epiphyseal cartilage (P3 knee cartilage) and 3-week high density chondrocyte cultures (culture day 21 neocartilage) (12). However, cartilage development *in vivo* involves environmental signals and factors such as mechanical loading that are absent *in vitro*. Meta-analysis of the *in vivo* and *in vitro*

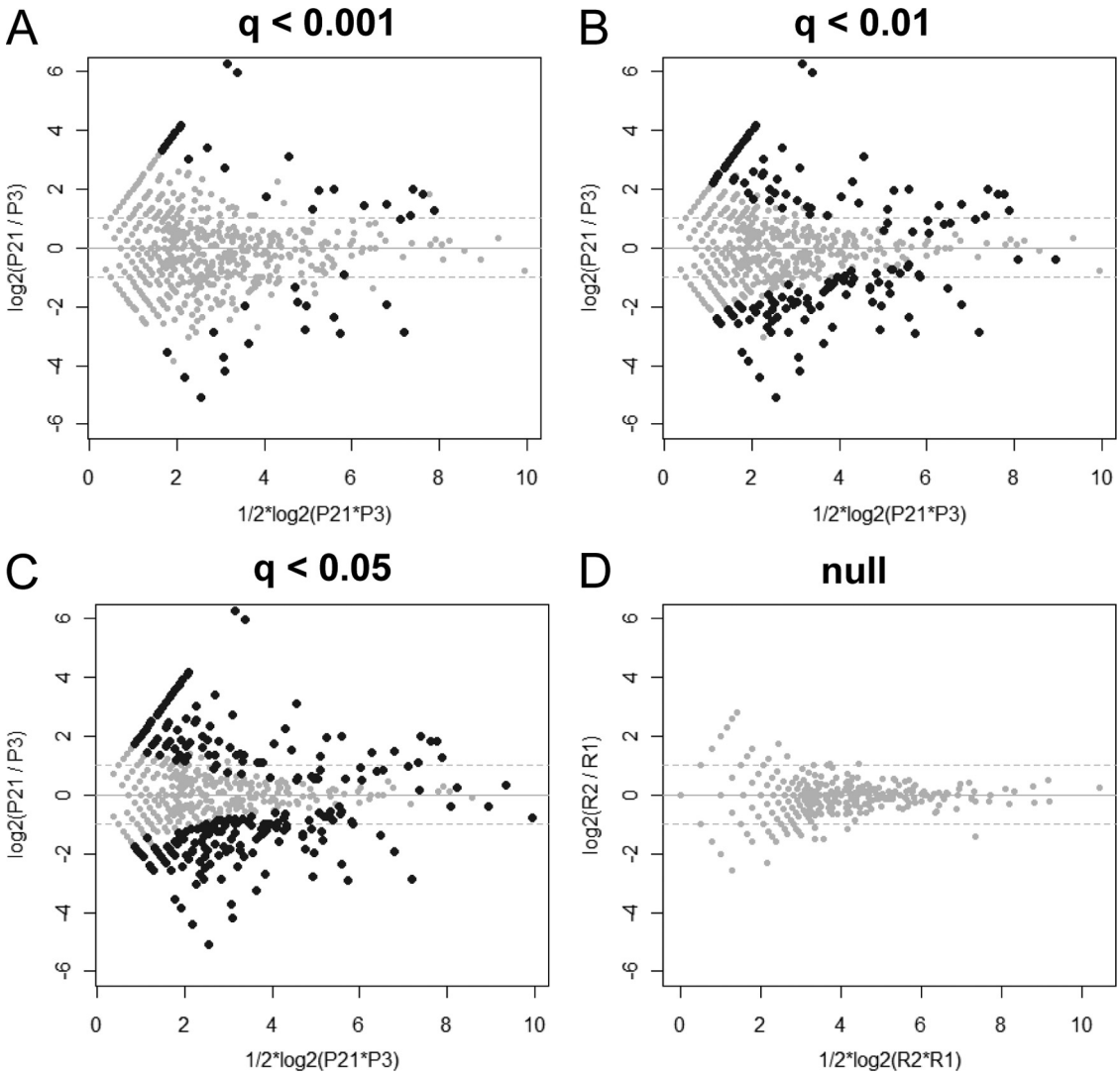

FIG. 4. **Global representation of the normalized protein counts for the P3 and P21 femoral head cartilage data set at three false discovery rates.** Each *data point* in the MA plot represents the relative abundance of a protein in P3 and P21 cartilage. Both axes are $\log_2$ transformed, where the *horizontal axis* represents the product of the spectral counts, and the *vertical axis* represents the ratio of the spectral counts. The *solid gray line* represents equal abundance, and the *dashed gray lines* represent a 2-fold difference in abundance. In *A–C*, the *black data points* represent proteins that have a significant difference in abundance. The number of significant proteins given *q* value thresholds of 0.001, 0.01, and 0.05 were 74, 146, and 282, respectively. *D*, a representative plot of two biological replicates (P3 replicates R1 and R2) to show the null distribution of proteins, *i.e.* those with no actual difference in abundance.

proteomics data sets was therefore used to: (i) identify potential components with specific roles *in vivo* and (ii) identify components that are involved in both processes and are therefore suitable candidates for further investigation *in vitro*.

To generate an equivalent data set for cartilage maturation *in vitro*, MS/MS data from our previous study (12) were searched against the *M. musculus* complete proteome set, resulting in 44,960 confident peptide-spectrum matches (FDR = 0.43%) and 839 protein identifications (supplemental Table 2*B*). Excluding eight contaminants, 102 proteins were significantly different between P3 knee cartilage and *in vitro* chondrocyte culture day 21 neocartilage extracts ($q < 0.01$), listed in supplemental Table 2*B*. Almost half of these proteins ($n = 45$) were also significant in femoral head cartilage maturation (highlighted in Fig. 6*A* and details provided in supplemental Table 2*C*). As an initial evaluation of the *in vitro* and *in vivo* proteomics data sets, protein subsets classified by the functional terms "extracellular matrix," "endoplasmic reticulum," and "ribonucleoprotein" were represented as MA plots (Fig. 6*B*). Consistent with the *in vivo* data set, most of the significant ER components and ribonucleoproteins *in vitro* were enriched in P3 cartilage. In addition, significant ECM components were evenly distributed above and below $y = 0$ both *in vitro* and *in vivo*.

To further investigate the similarities and differences between neocartilage formation and femoral head cartilage

TABLE I

Significant extracellular matrix and related proteins involved in cartilage development in vivo

Of the 146 proteins that were differentially expressed in P3 and P21 cartilage, a subset of 34 significant ($q < 0.01$) ECM and related proteins were annotated by the functional terms extracellular matrix (ECM), thrombospondin, type III repeat (TSP), EGF-like region, conserved site (EGF), leucine-rich repeat (LRR), polysaccharide binding (PSB), and positive regulation of cell adhesion (Adhesion). Classification of each entry is indicated by ×. Five additional extracellular proteins, thrombospondin-1 (Thbs1), thrombospondin-4 (Thbs4), lactadherin (Mfge8), lubricin (Prg4), and matrilin-4 (Matn4), were included as extracellular matrix-related components on the basis of their classification under one or more of the enriched functional terms.

Protein name	Gene name	Enriched functional terms						*q* value	Fold (P21/P3)	Accession number
		ECM	PSB	LRR	TSP	EGF	Adhesion			
Vitrin	Vit	×	×				×	0.00044	18.0	Q8VHI5
Osteomodulin	Omd	×		×				0.000594	17.3	O35103
Uncharacterized protein (cartilage intermediate matrix protein, isoform 2)	Cilp2[a]	×						0.001026	10.7	D3Z7H8
Thrombospondin 4	Thbs4				×	×		0.003841	10.7	P61750
Coiled-coil domain-containing protein 80 (Urb)	Ccdc80	×	×				×	0.000306	10.0	Q8R2G6
Uncharacterized protein (lubricin)	Prg4		×					0.00273	9.3	E0CZ58
SPARC	Sparc	×						0.000531	8.6	P07214
Tenascin X	Tnxb	×	×			×	×	0.005008	7.0	O35452
Collagen α-1(X) chain	Col10a1	×						0.000328	6.5	Q05306
α-2-HS-glycoprotein	Ahsg	×						0.00195	4.9	P29699
Fibromodulin	Fmod	×		×				0.00048	4.1	P50608
Decorin	Dcn	×	×	×				0.00044	3.9	P28654
Galectin-3	Lgals3	×						0.005544	3.8	P16110
Uncharacterized protein (lactadherin)	Mfge8					×		0.000123	3.8	E9QKW0
Collagen α-1(III) chain	Col3a1	×						0.007115	3.5	P08121
Cartilage oligomeric matrix protein	Comp	×	×		×	×		0.00209	3.4	Q9R0G6
Chondroadherin	Chad	×		×				6.29E-05	2.8	O55226
Fibronectin	Fn1	×	×			×		0.000537	2.8	P11276
Matrilin-3	Matn3	×				×		0.000323	2.4	Q543Q2
EMILIN-1	Emilin1	×					×	0.003753	2.4	Q99K41
Thrombospondin 1	Thbs1				×	×	×	0.002643	1.8	Q80YQ1
Proline arginine-rich end leucine-rich repeat	Prelp	×		×				0.002347	1.5	Q543S0
Aggrecan	Acan	×	×					0.00555	-1.3	E9QLS9
Matrilin-4	Matn4					×		0.00048	-1.9	O89029
Collagen α-3(IX) chain	Col9a3[a]	×						0.000954	-2.7	A2ACT7
Epiphycan	Epyc	×		×				0.001311	-2.7	P70186
Transforming growth factor, beta induced	Tgfbi	×						0.00209	-2.7	A1L353
Leprecan 1	Lepre1	×						0.003213	-2.8	A6PW84
Collagen α-2(IX) chain	Col9a2	×						0.000459	-3.6	Q07643
Collagen α-2(V) chain	Col5a2	×						0.00901	-3.8	Q3U962
Tenascin	Tnc	×				×		0.000185	-4	Q80YX1
Cartilage-associated protein	Crtap	×						0.005008	-5	Q8C8C5
Asporin	Aspn	×		×				0.009304	-5.7	A6H6K1
Collagen α-1(IX) chain	Col9a1	×						0.000185	-7.1	Q05722

[a] The 29 differentially abundant proteins classified as ECM components (GO:0031012) included Cilp2 and Col9a3, which are annotated as ECM based on the human homologues.

development, the list of significant proteins *in vitro* were submitted to DAVID for functional annotation (supplemental Table 3*B*). Several GO annotations enriched in the *in vitro* data set were similar to those enriched in the *in vivo* data set. In particular, the cellular component with the most entries was "extracellular matrix" ($n = 22$). Additional ECM-related terms associated with cartilage development both *in vivo* and *in vitro* included "polysaccharide binding" (cluster 4; $n = 8$), "thrombospondin, C-terminal" (cluster 7; $n = 3$), and "EGF-like, type 3" (cluster 9; $n = 7$). However, the ECM-related terms "lamin G, thrombospondin-type, N-terminal" (cluster 5; $n = 4$), "fibrillar collagen" (cluster 6; $n = 3$), and "von Willebrand factor, type C" (cluster 8; $n = 4$) were specifically enriched *in vitro*.

These results indicate fundamental roles for ECM components in cartilage development in both environments, but the

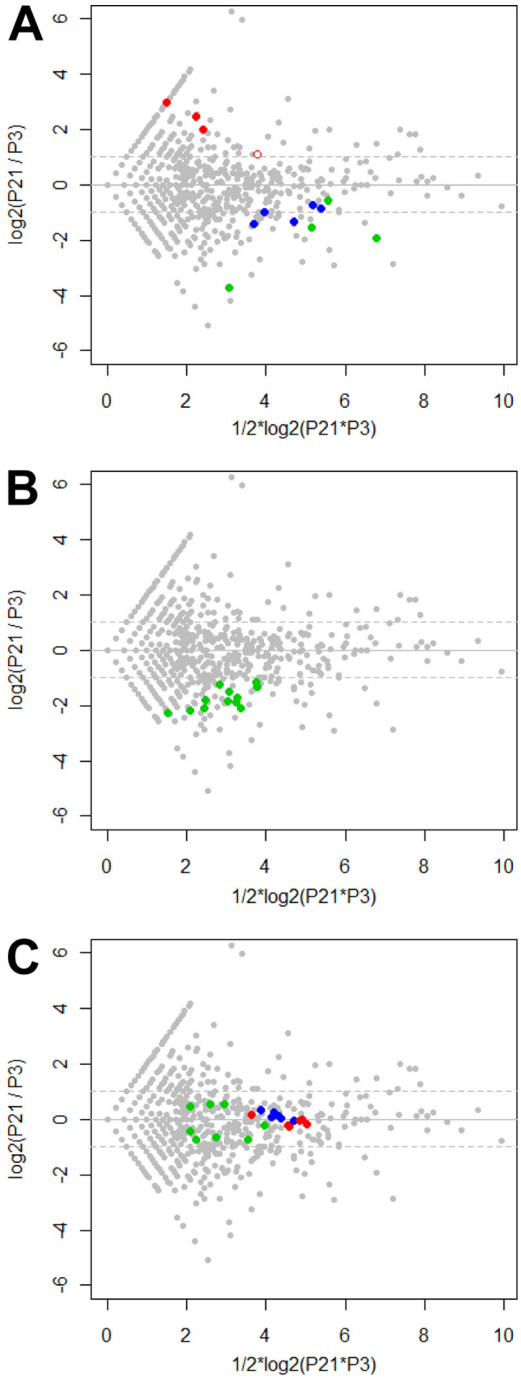

FIG. 5. **Functional groups associated with femoral head cartilage development.** Each *data point* in the plot represents the relative abundance of a protein between P3 and P21 cartilage, where proteins above the *horizontal axis* are more abundant at P21. Both axes are $\log_2$ transformed, where the *horizontal axis* represents the product of the spectral counts and the *vertical axis* represents the ratio of the spectral counts. In *A* and *B*, colored data points represent differentially abundant proteins ($q < 0.01$), and in *C*, none of the proteins have significant differences in abundance. *A*, three distinct protein groups associated with the endoplasmic reticulum: oxidoreductase activity proteins (Lepre1, Plod2, Plod1, P4ha1, and P4ha2) are highlighted as *green filled circles*, protein disulfide isomerase activity proteins (P4hb, Pdia3, Pdia4, and Pdia6) are highlighted as blue *filled circles*, and PIRSF036326:reticulocalbin proteins (Calu, Rcn1, and Rcn2) are highlighted as *red filled circles*. The fourth member of the reticulocalbin family identified (Rcn3) is highlighted as an *open red circle*. *B*, ribonucleoproteins (Hnrnpab, Hnrnpu, Rpl9, Rpl27a, Rps4x, Rps6, Rps8, Rpl4, Rpl6, Rpl32, Rps15, and Rpl22). *C*, housekeeping protein families that are not differentially abundant between P3 and P21 cartilage: the tubulin chains Tuba1b, Tuba1a, Tubb2a, Tubb2c, Tubb5, and Tubb6 (*red filled circles*); the 14-3-3 proteins Ywhaq, Ywhab, Ywhae, Ywhah, Ywhag, and Ywhaz (*blue filled circles*); and the t-complex chaperonin subunits Cct2, Cct3, Cct4, Cct5, Cct6a, Cct7, Cct8, and Tcp1 (*green filled circles*).

two processes are likely to involve distinct protein subsets. The 34 significant ECM and related proteins identified *in vivo* (Table I) and the 27 significant *in vitro* components belonging to the ECM and related GO terms described above were compared using Venn diagrams. Fig. 7*A* shows the protein significantly increased in abundance *in vitro* and/or *in vivo*, and Fig. 7*B* shows the proteins significantly decreased in abundance *in vitro* and/or *in vivo*.

Twenty-two ECM components were increased during cartilage development *in vivo* (group II+III). Of these, eight were also increased during cartilage maturation *in vitro* (group II). The remaining 14 proteins enriched in P21 femoral head cartilage (group III) could be subclassified into proteins that were also detected but not significantly increased during cartilage maturation *in vitro* ($n = 6$) and proteins that were detected exclusively *in vivo* ($n = 8$). For example, of the small leucine-rich repeat proteoglycans in group III, chondroadherin (Chad), fibromodulin (Fmod), proline arginine-rich end leucine-rich repeat protein (Prelp), and decorin (Dcn) were also detected in neocartilage cultures, whereas osteomodulin was detected *only* in P21 femoral head cartilage.

Twelve ECM and related proteins were significantly decreased in P21 cartilage relative to P3 cartilage (group V+VI), five of which were also down-regulated during cartilage ECM maturation *in vitro* (group V). This comparison highlights four key protein subsets: components that are increased during ECM development both *in vitro* and *in vivo* (group II), components that are associated in general with a less "mature" cartilage ECM (group V), and proteins involved in specific aspects of ECM development, either *in vitro* (group I) or *in vivo* (group III).

Immunohistochemical Analysis of Novel Proteins Associated with Maturation of the Extracellular Matrix—Chondrocyte hypertrophy and development of articular cartilage are the major histologic features of femoral head cartilage development (Fig. 2). The prototypic markers for these processes (collagen X and lubricin, respectively) were among the significant proteins identified by our proteomic analysis. In addition, ECM components with no known role in these processes were identified. Therefore, we used a complementary approach to validate our proteomics data and further investigate the region-specific expression patterns in femoral head cartilage. Three proteins that were only identified in P21 cartilage

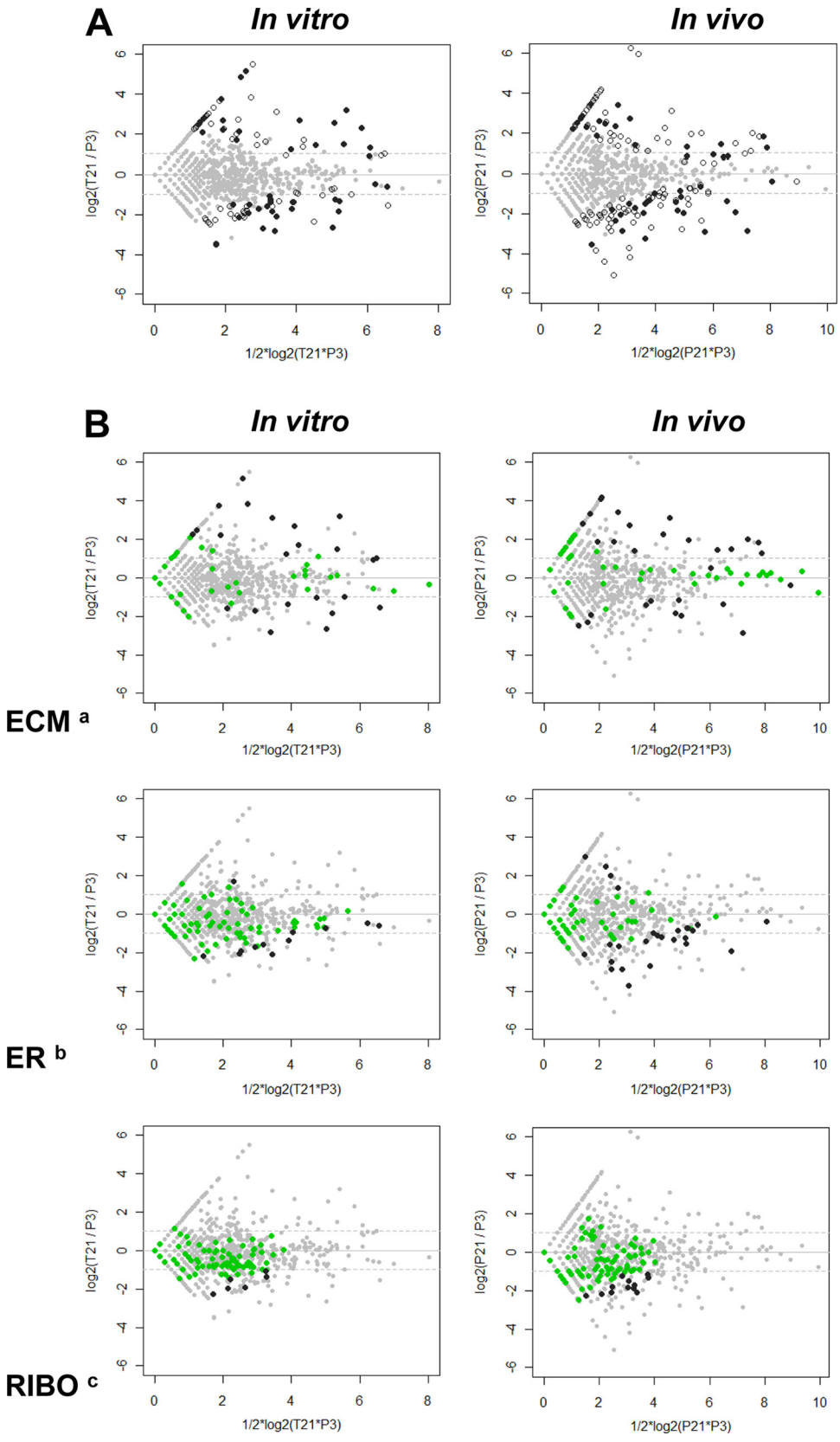
A
In vitro
In vivo
log2(T21 / P3)
log2(P21 / P3)
1/2*log2(T21*P3)
1/2*log2(P21*P3)
B
In vitro
In vivo
ECM a
ER b
RIBO c

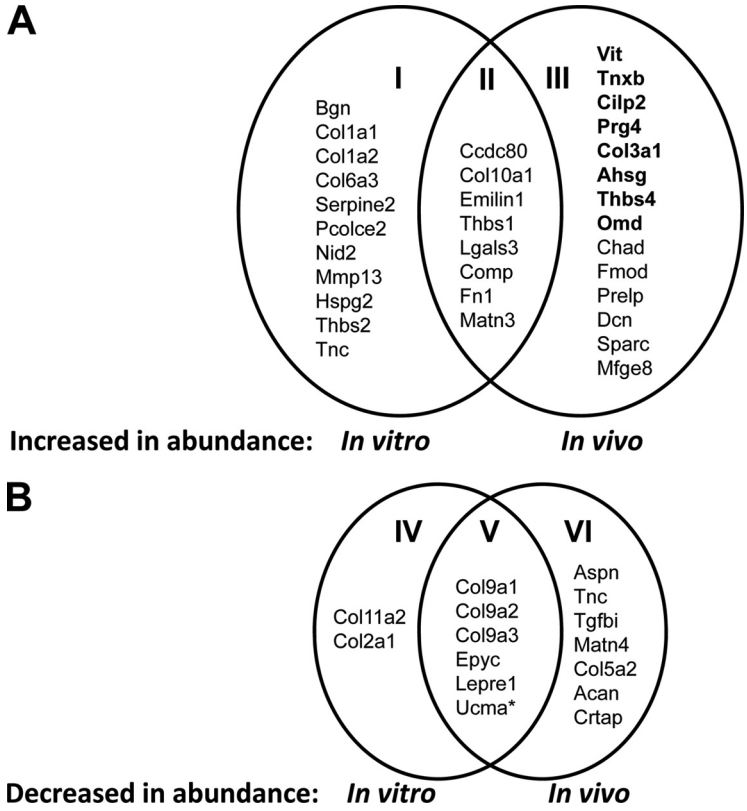

FIG. 7. **Comparison of extracellular matrix and related proteins involved in cartilage maturation *in vitro* and *in vivo*.** Proteins associated with cartilage maturation *in vitro* were identified by comparing P3 knee epiphyseal cartilage with neocartilage cultures. Of the differentially abundant proteins ($n = 102$), the proteins annotated by the significant functional terms extracellular matrix; polysaccharide binding; thrombospondin, C-terminal; EGF-like, type 3; lamin G, thrombospondin-type, N-terminal; fibrillar collagen; and von Willebrand factor, type C comprise the *in vitro* subsets. The proteins comprising the *in vivo* subsets are the ECM and matrix-related components associated with P3 and P21 femoral head cartilage development *in vivo* that are described in full in Table I. *A*, Venn diagram of the proteins *increased* during cartilage development specifically *in vitro* (*I*), specifically *in vivo* (*III*), or both *in vitro* and *in vivo* (*II*). The eight proteins in group III highlighted in *bold* were detected exclusively in P21 cartilage, whereas the remaining six proteins were also detected, but not significantly enriched, in neocartilage. *B*, Venn diagram of the proteins *decreased* during cartilage development specifically *in vitro* (*IV*), specifically *in vivo* (*VI*), or both *in vitro* and *in vivo* (*V*). Ucma (unique cartilage matrix associated protein) was included in group V because it was enriched in P3 cartilage in both comparisons; however, it was only statistically significant ($q < 0.01$) *in vitro*.

samples and therefore likely to be involved specifically in cartilage development *in vivo* (vitrin, tenascin X and CILP-2) and one protein that increased in abundance both *in vitro* and *in vivo* (Urb) were analyzed by immunohistochemistry. Antibodies for tenascin X did not give a reliable positive signal under the conditions tested; therefore only Urb, vitrin, and CILP-2 results are shown.

Analysis of Urb, vitrin, and CILP-2 in P3 cartilage revealed intracellular immunostaining of all three proteins, but little evidence of region-specific expression (Fig. 8*A*). In contrast, Urb, vitrin, and CILP-2 immunostaining in P21 cartilage was localized specifically with the ECM and chondrocyte populations of different maturation stages. Strong immunostaining for Urb was observed in the interterritorial matrix of the presumptive ossification center and the underlying clusters of maturing/prehypertrophic chondrocytes (Fig. 8*B*), but no signal was detected in proliferative growth plate cartilage matrix. Vitrin immunostaining overlapped with Urb expression in the

FIG. 6. **Global evaluation of *in vitro* and *in vivo* models of cartilage development.** MA plots of the *in vitro* (*left panels*) and *in vivo* (*right panels*) spectral count data. The *in vitro* spectral count data was based on the proteomic comparison of P3 mouse knee epiphyseal cartilage and neocartilage cultures (12), and the *in vivo* spectral count data is based on the P3 and P21 femoral head cartilage. The *horizontal axis* represents the product of the spectral counts, and the *vertical axis* represents the ratio of the spectral counts. Axes are $\log_2$ transformed. Proteins that are not differentially abundant are plotted as *gray filled circles*. *A*, proteins with significant differences in abundance ($q < 0.01$) either *in vitro* or *in vivo* are represented by *open circles*, and proteins that are differentially abundant in both developmental systems are represented as *black filled circles*. *B*, protein subsets *in vitro* and *in vivo* classified by the functional terms extracellular matrix (*ECM*), endoplasmic reticulum (*ER*), and ribonucleoprotein (*RIBO*) are highlighted as *filled circles*. Differentially abundant proteins are represented as *black filled circles*.

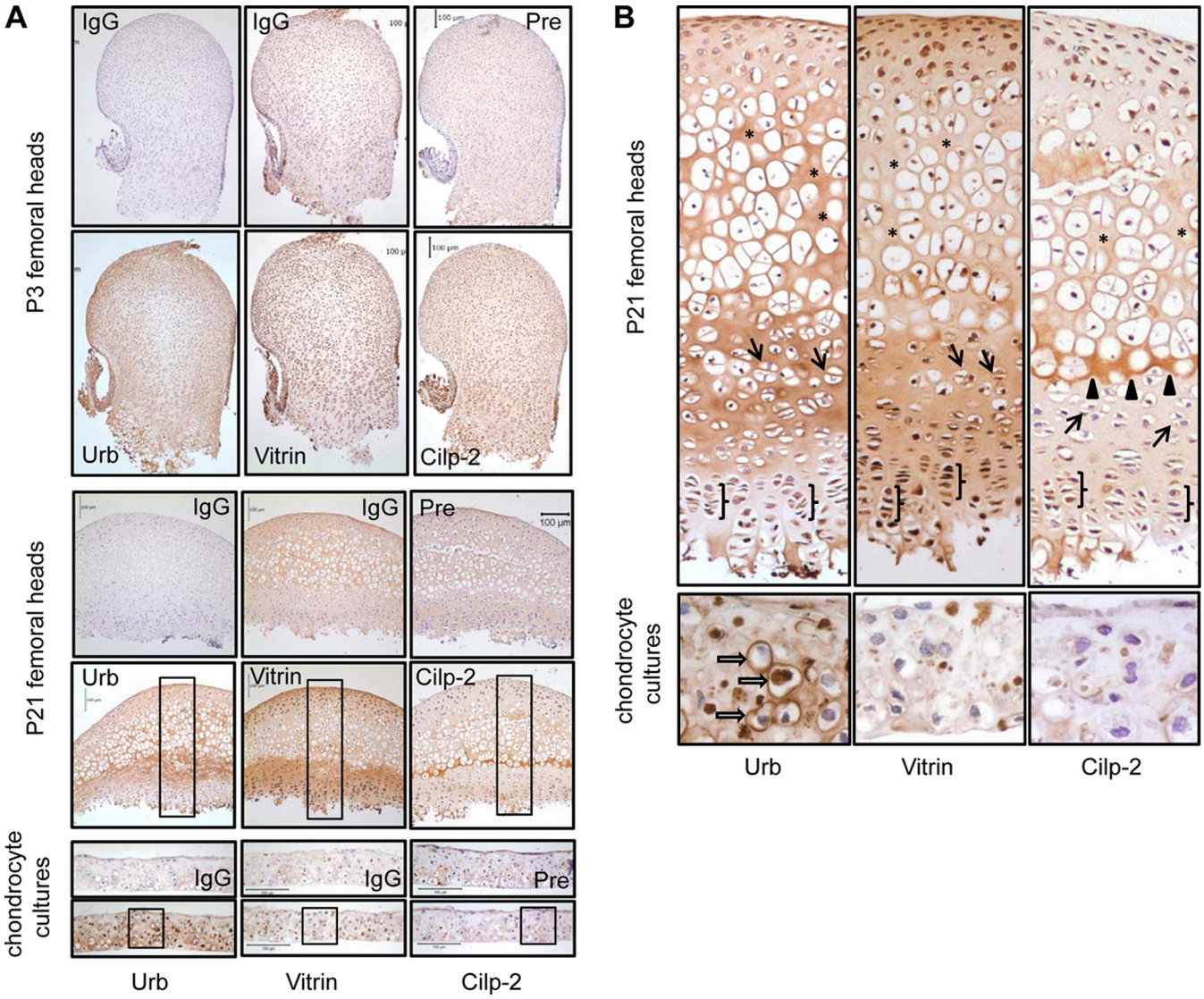

FIG. 8. **Immunohistochemistry of vitrin, Urb and CILP-2 in femoral head cartilage and 3-week neocartilage cultures.** *A*, saggittal paraffin sections of P3 and P21 femoral head cartilage and cryosections of 3-week chondrocyte neocartilage cultures were incubated with antibodies to Urb, vitrin, and CILP-2. Positive immunolocalization for the three proteins is indicated by *brown* staining, and histology/nuclear localization is indicated by *blue-violet* hematoxylin counter stain. *B*, expanded views of the *boxed regions* in *A*. The marked regions of the P21 femoral head cartilage correspond to the hypertrophic cartilage of the presumptive ossification center (*asterisks*), the region of maturing/prehypertrophic chondrocytes (*open arrows*), and columns of proliferative chondrocytes (*brackets*). The most intense region of CILP-2 staining at the margin of the presumptive ossification center and the underlying growth plate is marked with *filled triangles*. The most intense region of Urb staining in neocartilage cultures is indicated by *arrows*.

maturing/prehypertrophic region but was relatively much weaker in the hypertrophic cartilage of the presumptive ossification center. Strong vitrin expression was also observed in the proliferative zone from which Urb was absent. The immunopositive signal for CILP-2 was more restricted than vitrin and Urb, with a tight band of staining at the margin of the presumptive ossification center and the underlying growth plate. This pattern is consistent with the localized expression of CILP-2 in the calcified deeper zones of knee articular cartilage (22).

According to our proteomics analysis, Urb was detected both *in vitro* and *in vivo*, whereas CILP-2 and vitrin were only identified in P21 femoral head cartilage (Fig. 7). Consistent with these results, only Urb was detected in the ECM of chondrocyte neocartilage cultures (Fig. 8*A*). High magnification images of the chondrocyte cultures showed intracellular Urb staining and pericellular staining that was particularly strong in enlarged chondrocytes, most likely undergoing hypertrophy (Fig. 8*B*). These results support a role for Urb in chondrocyte hypertrophy, whereas the lack of CILP-2 and vitrin in neocartilage suggest roles in processes that are not recapitulated in culture. Collectively, the results of CILP-2, Urb, and vitrin analysis by immunohistochemistry agree

closely with the proteomics data and provide evidence for very distinct roles in cartilage development.

DISCUSSION

The formation of skeletal elements by endochondral ossification involves tightly regulated chondrocyte differentiation. In the mouse, this developmental process has been investigated "spatially " using microdissection and microarray analysis of chondrocyte populations from histomorphologically defined zones of growth plate cartilage (5–7). This is a challenging target for proteomics particularly because of the very limited amount of protein available from individual cartilage zones. To overcome this, we used a "temporal" approach based on developmental stages of femoral head cartilage with a high proportion of immature chondrocytes (day 3) or prehypertrophic and hypertrophic chondrocytes (day 21). Label-free quantitative mass spectrometry identified 703 proteins, of which 67 were significantly more abundant in P21 cartilage and 79 were more abundant in P3 cartilage ($q < 0.01$). The prototypic markers for chondrocyte differentiation (collagen X) and development of the articular surface (lubricin) were significantly enriched in P21 cartilage, demonstrating the utility of our model for discovery of new proteins and processes involved in cartilage development. The significance of our results is discussed below.

Overview of Significant Biological Processes and Protein Functional Categories Enriched in P3 and P21 Cartilage Extracts—The highest ranking protein functional category in femoral head cartilage development was extracellular matrix (GO:0031012), consistent with the increased abundance Gdn-HCl-extracted proteins relative to NaCl-extracted proteins in P21 cartilage (Fig. 3*B*). However, the significant proteins and protein functional classes in P3 and P21 cartilage proteomes reflected a complex tissue and cellular maturation process involving more than ECM biosynthesis. Proteins significantly enriched in P21 cartilage also included cytosolic (enolase and glyceraldehyde-3-phosphate dehydrogenase), mitochondrial (creatine kinase B), and structural (β-actin and vimentin) elements (supplemental Table 2*A*). Other cellular protein classes such as tubulins, t-complex chaperone subunits, and 14-3-3 proteins that were robustly expressed in P3 and P21 chondrocytes at approximately equal levels (Fig. 4*C*) could be regarded as performing "housekeeping " functions at both stages. Although many residents of the intracellular endomembrane system were significantly reduced in P21 cartilage, the reticulocalbin family of lumenal ER proteins strikingly reversed this trend. In addition, 12 of the significant extracellular or cell matrix components were more abundant in P3 cartilage, underlining the role of ECM remodeling, as well as synthesis, during the maturation process.

Novel Cell Adhesion Proteins and Evidence for Sushi Domain-mediated Interactions in Cartilage—Four of the significant proteins classified by the GO term "regulation of cell adhesion" are novel in the context of post-natal cartilage development (emilin-1, tenascin X, vitrin, and Urb). Urb and vitrin were previously identified by *in silico* screening for novel ECM components and verified as promoting cell attachment and matrix assembly *in vitro* (21). The diffuse immunostaining for Urb throughout P3 cartilage is consistent with observations in mouse embryonic ribs and vertebrae (21, 32). The restricted Urb expression within the prehypertrophic cartilage and presumptive ossification center at P21 suggests a role in the ECM prior to bone formation. In addition, the "extraction profile" (the distribution between readily soluble and guanidine-soluble P3 and P21 extracts) of Urb was consistent with the integration of Urb within the ECM during cartilage development (data not shown).

Urb is a member of the sushi repeat-containing protein superfamily. The sushi domain, also known as a complement control protein module, is a structural motif of ~60 amino acids that mediates protein-protein interactions. We identified three further sushi repeat proteins that have not previously been reported in cartilage at the protein level. Fibulin-7 (Fbln7), the only fibulin with a sushi repeat domain, has been detected in growth plate and articular cartilage at the mRNA level (33), whereas the X-linked sushi repeat containing protein (Srpx) and homolog (Srpx2) are entirely novel cartilage components. Preliminary studies in our lab showed similar localization of Srpx2 expression in P21 cartilage to that of Urb (data not shown). The identification of ligands for these sushi domain-containing secreted proteins will help elucidate their roles in cell attachment and/or matrix protein assembly in cartilage.

The dramatic increase in vitrin abundance during femoral head cartilage development was unexpected. Vitrin is a modular protein containing two von Willebrand factor A domains at the C terminus that forms a separate subfamily of noncollagenous A domain-containing proteins related to the matrilins (34). The role of matrilins in bridging the collagen and proteoglycan macromolecular networks in cartilage is well known, whereas little has been reported on vitrin function since its discovery in bovine vitreous (35). Localization of vitrin by immunohistochemistry revealed particularly strong staining in the proliferative region of the P21 growth plate cartilage, from which Urb staining was absent. Also unlike Urb, vitrin was more abundant in the matrix surrounding the prehypertrophic chondrocytes than in the adjacent hypertrophic cartilage. Consistent with this region-specific pattern, the transition from prehypertrophic to hypertrophic chondrocytes in the growth plate is marked by a 10-fold decrease in vitrin mRNA.[2] This tightly regulated expression signifies a potential role in maintaining ECM structure in the proliferative and prehypertrophic cartilage matrix, making vitrin a novel candidate for human chondrodysplasias and an important target for further analysis *in vivo*.

[2] D. Belluoccio, and J. F. Bateman, unpublished observations.

Similarities between Femoral Head Cartilage Development and Neocartilage Formation in Vitro—Our previous investigation of cartilage matrix formation in chondrocyte "neocartilage" cultures identified a cohort of ECM components based on differential protein solubility compared with P3 mouse knee epiphyseal cartilage (12). Meta-analysis of the two model systems revealed matrix components and cell adhesion proteins that were significant both *in vitro* and *in vivo*. These included matrilin-3 (Matn3), COMP, thrombospondin-1 (Thbs1), and fibronectin (Fn1), supporting fundamental roles for these components in ECM network formation and tissue stability in cartilage (36).

Chondrocyte hypertrophy and associated ECM remodeling creates the niche for vascular invasion and replacement of the cartilage remnants with bone. In addition to this developmental role, hypertrophy of articular chondrocytes in osteoarthritis leads to neovascularization and osteophyte formation (37). Our proteomics analysis provided evidence for chondrocyte hypertrophy in both femoral head cartilage development and in neocartilage. In addition to collagen X, the cardinal marker of late stage chondrocyte differentiation, lesser known components of hypertrophic cartilage such as annexin VIII (Anxa8), galectin-3 (Lgals3), and lysyl oxidase C (Loxl4) (38) were all significantly increased. The reduction in collagen IX α1, α2, and α3 chains extracted from P21 cartilage suggests an inverse relationship between collagen IX and collagen X synthesis. Epiphycan (Epyc) and unique cartilage matrix-associated protein (Ucma), two known markers for immature chondrocytes (39, 40), were also enriched in P3 cartilage relative to P21 cartilage. The relative abundance of these differentiation markers in P3 and P21 cartilage, consistent with their expression changes *in vitro*, reveals key similarities in matrix development and remodeling *in vitro* and *in vivo*.

Specific and Novel Proteins Involved in Femoral Head Cartilage Development—We anticipated that cartilage development *in vivo* would involve specific proteins related to the unique physiological conditions in the developing joint that cannot be recapitulated in chondrocyte cultures. In support of this hypothesis, eight of the P21-enriched ECM and matrix-related proteins in Table I were specific to femoral head cartilage development (Fig. 6, group III), including the articular cartilage superficial zone proteoglycan lubricin (Prg4). Another component detected only in P21 cartilage was CILP-2, a recently described isoform of the cartilage intermediate layer protein (CILP-1) (41). Whereas CILP-1 expression is restricted to the middle layer of articular cartilage, CILP-2 is differentially expressed in the meniscus and deeper articular cartilage zones of the knee joint (22). In the P21 femoral head, the highly localized band of CILP-2 expression at the margin of the hypertrophic cartilage and underlying growth plate provides further evidence for a specialized role in the ECM during cartilage development *in vivo*.

Tenascin X was only associated with cartilage development *in vivo* and has not previously been detected in cartilage. Tenascin X deficiency in humans and mice results in Ehlers-Danlos syndrome caused by abnormal collagen fibrillogenesis in skin and muscle (42, 43), raising the possibility of a similar function in cartilage. In developing heart and skeletal muscle, the reciprocal expression of tenascin X and tenascin C led to the suggestion that they perform nonredundant functions (44). Interestingly, we observed a similar reciprocal relationship between tenascin X expression and tenascin C, a marker of early chondrogenesis (45).

Matrix constituents that were specifically decreased *in vivo* included the transforming growth factor β1 (TGFβ1)-regulated proteins, tenascin C, asporin, and TGFβ-induced ig-h3 (46–48). These results support a role for TGFβ1 signaling during early cartilage development *in vivo*, consistent with the positive effect of TGFβ1 on the differentiation of mesenchymal chondrocyte precursors *in vitro* (49, 50). Altered TGFβ1 signaling is implicated in cartilage degeneration associated with aging and arthritis (51), and pathologic changes in cartilage homeostasis and chondrocyte phenotype include re-expression of early markers of cartilage development. Of the TGFβ-regulated proteins enriched in P3 cartilage, asporin and tenascin C are absent from normal adult cartilage but expressed in osteoarthritis, whereas TGFβ-induced ig-h3 warrants investigation as a potential novel biomarker.

The overlap in protein expression between terminally differentiated chondrocytes and osteoblasts at the chondro-osseous junction has generated debate over chondrocyte fate and the respective roles of chondrocytes and osteoblasts in mineralization of the hypertrophic cartilage (reviewed in Ref. 52). Osteomodulin was detected exclusively in P21 femoral head cartilage and so is potentially a product of osteoblasts recruited into the hypertrophic cartilage. In contrast, three proteins involved in normal and pathologic mineralization of the cartilage matrix that were enriched in P21 cartilage (alkaline phosphatase/Alpal, osteopontin/Spp1 and osteonectin/Sparc) are also synthesized by chondrocytes in culture (53–55). Further analysis of these constituents *in vitro* and *in vivo* will determine their cellular origin and elucidate their roles in late stage chondrocyte differentiation and hypertrophic cartilage mineralization.

Regulation of Specific Endoplasmic Reticulum-resident Proteins and Elements of the Secretory Protein Trafficking and Quality Control System—Development of the cartilage ECM during endochondral ossification is essential for tissue integrity and normal chondrocyte differentiation, and we have identified new components involved in matrix development *in vivo*. In addition to changes in the cartilage matrix proteome, which are the net result of protein accumulation and turnover, we identified changes in ER proteins involved in matrix protein biosynthesis. In particular, cartilage maturation was accompanied by changes in the repertoire of enzymes and molecular chaperones involved in the post-translational modification, folding, and assembly cartilage collagens.

One significant group of proteins enriched in P3 cartilage belong to the iron-dependent dioxygenases, specifically five members of the prolyl 3-hydroxylase, prolyl 4-hydroxylase, and lysyl hydroxylase families, which catalyze post-translation modification of collagen α chains. Prolyl 4-hydroxylation of the Xaa-Pro-Gly collagen tripeptide repeat is essential for triple helical stability, whereas lysyl hydroxylation of Xaa-Lys-Gly generates carbohydrate attachment sites that stabilize intermolecular collagen interactions. Both prolyl 4-hydroxylase α subunit isoforms (P4ha1 and P4ha2), two lysyl hydroxylases (Plod1 and Plod2), and the procollagen galactosyl transferase-1 (Glt25d1) were significantly more abundant in P3 cartilage. A further modification essential for collagen triple helix formation is the *cis-trans* isomerization of peptidyl prolyl bonds. In our study, two ER-associated peptidyl prolyl *cis-trans* isomerases, Fkbp10 and Ppib, were significantly more abundant in P3 chondrocytes, whereas levels of the cytosolic enzymes Ppia and Ppic were unchanged.

Prolyl 3-hydroxylation, a highly site-specific modification of collagen α chains, appears to regulate the transit of correctly folded procollagen from the ER, in addition to proposed structural roles (56). Prolyl 3-hydroxylase 1 (Lepre1) combines with Ppib and cartilage-associated protein (Crtap) to form a chaperone complex that is critical for the quality control of collagen secretion. Mutations in any one of these subunits cause severe bone, tendon, and skin phenotypes in mice and osteogenesis imperfecta in humans (57, 58). Strikingly, all three components were more abundant in P3 cartilage, signifying an important developmental role for this complex in the assembly and secretion of cartilage collagens. Another ER chaperone involved in collagen-specific quality control, Hsp47 (Serpinh1), has also recently been associated with osteogenesis imperfecta (59). Hsp47 was detected at high levels in P3 and P21 chondrocytes, albeit 1.3-fold reduced at P21, suggesting that Hsp47 is required throughout chondrocyte maturation. Although development of the cartilage ECM is marked by increased levels of certain collagen subtypes (*e.g.* collagen X) and a decrease in others (*e.g.* collagen IX), our results indicate that collagen biosynthesis is highest overall during early stages of cartilage maturation.

The changing secretory function of the chondrocyte was also marked by reduced levels of protein disulfide isomerase (P4hb), Pdia3, Pdia4, and Pdia6, indicating reduced capacity for folding and assembly of disulfide-linked proteins in the ER of late stage chondrocytes. The chaperone activity of Pdia4 (ERp72) is of particular interest because ERp72 forms stable complexes with disease-causing COMP and matrilin-3 mutants. Accumulation of these complexes in dilated ER cisternae is a hallmark of multiple epiphyseal dysplasia and pseudoachondroplasia (60–62), and the resulting ER stress affects normal chondrocyte differentiation and organization in the growth plate (63–65). ER stress induced by misfolding of collagen X in hypertrophic chondrocytes also contributes to the pathology of Schmid metaphyseal chondrodysplasia, type Schmid (66, 67), but the role of specific ER chaperones is not known. Although ERp72 was significantly reduced at P21, the master regulator of the unfolded protein response BiP (Hspa5) was detected at approximately equal levels in P3 and P21 cartilage. The changing repertoire of ER chaperones during the chondrocyte lifespan, and thus potential mechanisms of ER stress, may alter the impact of different disease-causing mutations on chondrocyte function.

Further biochemical evidence of changing ER function during chondrocyte differentiation was reflected in the significant increased in P21 cartilage of the reticulocalbins Rcn1, Rcn2, and Calu (reviewed in Ref. 68). Reticulocalbins are thought to regulate calcium-dependent functions in the ER and secretory pathway on the basis of ER retention motifs and multiple EF hand domains. However, their roles in chondrocytes are presently unknown. Collectively, our results reveal the down-regulation of secretory pathway elements related to collagen biosynthesis but a significant increase of the reticulocalbins. It has been reported that the cytosolic concentration of calcium increases with respect to chondrocyte maturation (69). Whether the reticulocalbins modify the bioavailability of ER lumenal calcium during cartilage development is a target for future studies.

Benefits of Our Approach and Future Perspectives—Endochondral ossification is a complex and fundamentally important developmental process that is difficult to study *in vitro* because of the interdependence of chondrocyte phenotype and tissue architecture. Using femoral head cartilage to investigate this process within its physiological context is both a strength and, because of increased complexity, a limitation. However, the integrated analysis of the *in vitro* and *in vivo* proteomic data sets enabled us to discover novel components, characterize the two developmental systems in greater detail, and pinpoint targets for further analysis. The expression and observed distribution of Urb supports a role in chondrocyte hypertrophy *in vitro* and *in vivo*, whereas the immunohistochemistry and proteomics data signified more specialized roles for vitrin and CILP-2 in cartilage development *in vivo*. Using this approach in cartilage from knockout mice and models of human skeletal dysplasias will enable proteomics level investigation of the roles of specific cartilage components and effects of disease-causing mutations on skeletal development *in vivo*.

Acknowledgment—We thank Anders Diseberg for analyzing the cartilage protein extracts by tandem mass spectrometry.

* This work was supported by National Health and Medical Research Council of Australia Grant 419237 and Deutsche Forschungsgemeinschaft Grants BR2304/5-1, BR2304/7-1, and SFB 829-B6. The project was also supported by the Victorian Government's Operational Infrastructure Support Program and was undertaken using infrastructure provided by the Australian Government through the National Collaborative Research Infrastructure Strategy and Bioplatforms Australia. The costs of publication of this article were defrayed in part by the payment of page charges. This article must therefore be

hereby marked "*advertisement*" in accordance with 18 U.S.C. Section 1734 solely to indicate this fact.

[S] This article contains supplemental Tables 1–3.

¶ To whom correspondence may be addressed: Central Science Laboratory, Bag 74, University of Tasmania, Hobart, TAS 7001, Australia. Fax: 61-3-6226-2494; E-mail: richard.wilson@utas.edu.au.

*** To whom correspondence may be addressed: Murdoch Childrens Research Institute, Royal Children's Hospital, Parkville, Melbourne, VIC 3052, Australia. Fax: 61-3-8341-6429; E-mail: john.bateman@mcri.edu.au.

REFERENCES

1. Kronenberg, H. M. (2003) Developmental regulation of the growth plate. *Nature.* **423,** 332–336
2. Newman, B., and Wallis, G. A. (2003) Skeletal dysplasias caused by a disruption of skeletal patterning and endochondral ossification. *Clin. Genet.* **63,** 241–251
3. Behonick, D. J., and Werb, Z. (2003) A bit of give and take: The relationship between the extracellular matrix and the developing chondrocyte. *Mech. Dev.* **120,** 1327–1336
4. Bateman, J. F., Boot-Handford, R. P., and Lamandé, S. R. (2009) Genetic diseases of connective tissues: Cellular and extracellular effects of ECM mutations. *Nat. Rev. Genet.* **10,** 173–183
5. Belluoccio, D., Bernardo, B. C., Rowley, L., and Bateman, J. F. (2008) A microarray approach for comparative expression profiling of the discrete maturation zones of mouse growth plate cartilage. *Biochim. Biophys. Acta* **1779,** 330–340
6. Wang, Y., Middleton, F., Horton, J. A., Reichel, L., Farnum, C. E., and Damron, T. A. (2004) Microarray analysis of proliferative and hypertrophic growth plate zones identifies differentiation markers and signal pathways. *Bone* **35,** 1273–1293
7. James, C. G., Stanton, L. A., Agoston, H., Ulici, V., Underhill, T. M., and Beier, F. (2010) Genome-wide analyses of gene expression during mouse endochondral ossification. *PLoS One* **5,** e8693
8. Wilson, R. (2010) The extracellular matrix: An underexplored but important proteome. *Expert Rev. Proteomics* **7,** 803–806
9. Belluoccio, D., Wilson, R., Thornton, D. J., Wallis, T. P., Gorman, J. J., and Bateman, J. F. (2006) Proteomic analysis of mouse growth plate cartilage. *Proteomics* **6,** 6549–6553
10. Pecora, F., Forlino, A., Gualeni, B., Lupi, A., Giorgetti, S., Marchese, L., Stoppini, M., Tenni, R., Cetta, G., and Rossi, A. (2007) A quantitative and qualitative method for direct 2-DE analysis of murine cartilage. *Proteomics* **7,** 4003–4007
11. Vincourt, J. B., Lionneton, F., Kratassiouk, G., Guillemin, F., Netter, P., Mainard, D., and Magdalou, J. (2006) Establishment of a reliable method for direct proteome characterization of human articular cartilage. *Mol. Cell Proteomics* **5,** 1984–1995
12. Wilson, R., Diseberg, A. F., Gordon, L., Zivkovic, S., Tatarczuch, L., Mackie, E. J., Gorman, J. J., and Bateman, J. F. (2010) Comprehensive profiling of cartilage extracellular matrix formation and maturation using sequential extraction and label-free quantitative proteomics. *Mol. Cell. Proteomics* **9,** 1296–1313
13. Wilson, R., and Bateman, J. F. (2008) A robust method for proteomic characterization of mouse cartilage using solubility-based sequential fractionation and two-dimensional gel electrophoresis. *Matrix Biol.* **27,** 709–712
14. Wilson, R., Belluoccio, D., and Bateman, J. F. (2008) Proteomic analysis of cartilage proteins. *Methods* **45,** 22–31
15. Searle, B. C. (2010) Scaffold: A bioinformatic tool for validating MS/MS-based proteomic studies. *Proteomics* **10,** 1265–1269
16. Keller, A., Nesvizhskii, A. I., Kolker, E., and Aebersold, R. (2002) Empirical statistical model to estimate the accuracy of peptide identifications made by MS/MS and database search. *Anal. Chem.* **74,** 5383–5392
17. Nesvizhskii, A. I., Keller, A., Kolker, E., and Aebersold, R. (2003) A statistical model for identifying proteins by tandem mass spectrometry. *Anal. Chem.* **75,** 4646–4658
18. Pham, T. V., Piersma, S. R., Warmoes, M., and Jimenez, C. R. (2010) On the beta-binomial model for analysis of spectral count data in label-free tandem mass spectrometry-based proteomics. *Bioinformatics* **26,** 363–369
19. Käll, L., Storey, J. D., and Noble, W. S. (2009) QVALITY: Non-parametric estimation of q-values and posterior error probabilities. *Bioinformatics* **25,** 964–966
20. Huang da, W., Sherman, B. T., and Lempicki, R. A. (2009) Systematic and integrative analysis of large gene lists using DAVID bioinformatics resources. *Nat. Protoc.* **4,** 44–57
21. Manabe, R., Tsutsui, K., Yamada, T., Kimura, M., Nakano, I., Shimono, C., Sanzen, N., Furutani, Y., Fukuda, T., Oguri, Y., Shimamoto, K., Kiyozumi, D., Sato, Y., Sado, Y., Senoo, H., Yamashina, S., Fukuda, S., Kawai, J., Sugiura, N., Kimata, K., Hayashizaki, Y., and Sekiguchi, K. (2008) Transcriptome-based systematic identification of extracellular matrix proteins. *Proc. Natl. Acad. Sci. U.S.A.* **105,** 12849–12854
22. Bernardo, B. C., Belluoccio, D., Rowley, L., Little, C. B., Hansen, U., and Bateman, J. F. (2011) Cartilage Intermediate Layer Protein 2 (CILP-2) is expressed in articular and meniscal cartilage and down-regulated in experimental osteoarthritis. *J. Biol. Chem.* **286,** 37758–37767
23. Blumer, M. J., Longato, S., Schwarzer, C., and Fritsch, H. (2007) Bone development in the femoral epiphysis of mice: The role of cartilage canals and the fate of resting chondrocytes. *Dev. Dyn.* **236,** 2077–2088
24. Hankenson, K. D., Hormuzdi, S. G., Meganck, J. A., and Bornstein, P. (2005) Mice with a disruption of the thrombospondin 3 gene differ in geometric and biomechanical properties of bone and have accelerated development of the femoral head. *Mol. Cell. Biol.* **25,** 5599–5606
25. Stanton, H., Golub, S. B., Rogerson, F. M., Last, K., Little, C. B., and Fosang, A. J. (2011) Investigating ADAMTS-mediated aggrecanolysis in mouse cartilage. *Nat. Protoc.* **6,** 388–404
26. Sun, Y., Ma, S., Zhou, J., Yamoah, A. K., Feng, J. Q., Hinton, R. J., and Qin, C. (2010) Distribution of small integrin-binding ligand, N-linked glycoproteins (SIBLING) in the articular cartilage of the rat femoral head. *J. Histochem. Cytochem.* **58,** 1033–1043
27. Belluoccio, D., Etich, J., Rosenbaum, S., Frie, C., Grskovic, I., Stermann, J., Ehlen, H., Vogel, S., Zaucke, F., von der Mark, K., Bateman, J. F., and Brachvogel, B. (2010) Sorting of growth plate chondrocytes allows the isolation and characterization of cells of a defined differentiation status. *J. Bone Miner. Res.* **25,** 1267–1281
28. Storey, J. D., and Tibshirani, R. (2003) Statistical significance for genome-wide studies. *Proc. Natl. Acad. Sci. U.S.A.* **100,** 9440–9445
29. Quackenbush, J. (2002) Microarray data normalization and transformation. *Nat. Genet.* **32,** (suppl.) 496–501
30. Miller, R. R., and McDevitt, C. A. (1995) Thrombospondin 1 binds to the surface of bovine articular chondrocytes by a linear RGD-dependent mechanism. *FEBS Lett.* **363,** 214–216
31. Myllyharju, J., and Kivirikko, K. I. (2004) Collagens, modifying enzymes and their mutations in humans, flies and worms. *Trends Genet.* **20,** 33–43
32. Liu, Y., Monticone, M., Tonachini, L., Mastrogiacomo, M., Marigo, V., Cancedda, R., and Castagnola, P. (2004) URB expression in human bone marrow stromal cells and during mouse development. *Biochem. Biophys. Res. Commun.* **322,** 497–507
33. de Vega, S., Iwamoto, T., Nakamura, T., Hozumi, K., McKnight, D. A., Fisher, L. W., Fukumoto, S., and Yamada, Y. (2007) TM14 is a new member of the fibulin family (fibulin-7) that interacts with extracellular matrix molecules and is active for cell binding. *J. Biol. Chem.* **282,** 30878–30888
34. Whittaker, C. A., and Hynes, R. O. (2002) Distribution and evolution of von Willebrand/integrin A domains: Widely dispersed domains with roles in cell adhesion and elsewhere. *Mol. Biol. Cell.* **13,** 3369–3387
35. Mayne, R., Ren, Z. X., Liu, J., Cook, T., Carson, M., and Narayana, S. (1999) VIT-1: The second member of a new branch of the von Willebrand factor A domain superfamily. *Biochem. Soc. Trans.* **27,** 832–835
36. Heinegård, D., and Saxne, T. (2011) The role of the cartilage matrix in osteoarthritis. *Nat. Rev. Rheumatol.* **7,** 50–56
37. Dreier, R. (2010) Hypertrophic differentiation of chondrocytes in osteoarthritis: The developmental aspect of degenerative joint disorders. *Arthritis Res. Ther.* **12,** 216
38. White, A. H., Watson, R. E., Newman, B., Freemont, A. J., and Wallis, G. A. (2002) Annexin VIII is differentially expressed by chondrocytes in the mammalian growth plate during endochondral ossification and in osteoarthritic cartilage. *J. Bone Miner. Res.* **17,** 1851–1858
39. Johnson, H. J., Rosenberg, L., Choi, H. U., Garza, S., Höök, M., and Neame, P. J. (1997) Characterization of epiphycan, a small proteoglycan

with a leucine-rich repeat core protein. *J. Biol. Chem.* **272,** 18709–18717
40. Surmann-Schmitt, C., Dietz, U., Kireva, T., Adam, N., Park, J., Tagariello, A., Onnerfjord, P., Heinegård, D., Schlötzer-Schrehardt, U., Deutzmann, R., von der Mark, K., and Stock, M. (2008) Ucma, a novel secreted cartilage-specific protein with implications in osteogenesis. *J. Biol. Chem.* **283,** 7082–7093
41. Lorenzo, P., Bayliss, M. T., and Heinegård, D. (1998) A novel cartilage protein (CILP) present in the mid-zone of human articular cartilage increases with age. *J. Biol. Chem.* **273,** 23463–23468
42. Mao, J. R., Taylor, G., Dean, W. B., Wagner, D. R., Afzal, V., Lotz, J. C., Rubin, E. M., and Bristow, J. (2002) Tenascin-X deficiency mimics Ehlers-Danlos syndrome in mice through alteration of collagen deposition. *Nat. Genet.* **30,** 421–425
43. Burch, G. H., Gong, Y., Liu, W., Dettman, R. W., Curry, C. J., Smith, L., Miller, W. L., and Bristow, J. (1997) Tenascin-X deficiency is associated with Ehlers-Danlos syndrome. *Nat. Genet.* **17,** 104–108
44. Matsumoto, K., Saga, Y., Ikemura, T., Sakakura, T., and Chiquet-Ehrismann, R. (1994) The distribution of tenascin-X is distinct and often reciprocal to that of tenascin-C. *J. Cell Biol.* **125,** 483–493
45. Mackie, E. J., Thesleff, I., and Chiquet-Ehrismann, R. (1987) Tenascin is associated with chondrogenic and osteogenic differentiation *in vivo* and promotes chondrogenesis *in vitro*. *J. Cell Biol.* **105,** 2569–2579
46. Kou, I., Nakajima, M., and Ikegawa, S. (2007) Expression and regulation of the osteoarthritis-associated protein asporin. *J. Biol. Chem.* **282,** 32193–32199
47. Skonier, J., Bennett, K., Rothwell, V., Kosowski, S., Plowman, G., Wallace, P., Edelhoff, S., Disteche, C., Neubauer, M., Marquardt, H., et al. (1994) Beta ig-h3: A transforming growth factor-beta-responsive gene encoding a secreted protein that inhibits cell attachment in vitro and suppresses the growth of CHO cells in nude mice. *DNA Cell Biol.* **13,** 571–584
48. Qi, W. N., and Scully, S. P. (1997) Extracellular collagen modulates the regulation of chondrocytes by transforming growth factor-beta 1. *J Orthop Res.* **15,** 483–490
49. Han, F., Adams, C. S., Tao, Z., Williams, C. J., Zaka, R., Tuan, R. S., Norton, P. A., and Hickok, N. J. (2005) Transforming growth factor-beta1 (TGF-beta1) regulates ATDC5 chondrogenic differentiation and fibronectin isoform expression. *J. Cell. Biochem.* **95,** 750–762
50. Johnstone, B., Hering, T. M., Caplan, A. I., Goldberg, V. M., and Yoo, J. U. (1998) *In vitro* chondrogenesis of bone marrow-derived mesenchymal progenitor cells. *Exp. Cell. Res.* **238,** 265–272
51. van der Kraan, P. M., Blaney Davidson, E. N., and van den Berg, W. B. (2010) A role for age-related changes in TGFbeta signaling in aberrant chondrocyte differentiation and osteoarthritis. *Arthritis Res. Ther.* **12,** 201–210
52. Gerstenfeld, L. C., and Shapiro, F. D. (1996) Expression of bone-specific genes by hypertrophic chondrocytes: Implication of the complex functions of the hypertrophic chondrocyte during endochondral bone development. *J. Cell. Biochem.* **62,** 1–9
53. Chandrasekhar, S., Harvey, A. K., Johnson, M. G., and Becker, G. W. (1994) Osteonectin/SPARC is a product of articular chondrocytes/cartilage and is regulated by cytokines and growth factors. *Biochim. Biophys. Acta* **1221,** 7–14
54. Xu, Y., Pritzker, K. P., and Cruz, T. F. (1994) Characterization of chondrocyte alkaline phosphatase as a potential mediator in the dissolution of calcium pyrophosphate dihydrate crystals. *J. Rheumatol.* **21,** 912–919
55. Rosenthal, A. K., Gohr, C. M., Uzuki, M., and Masuda, I. (2007) Osteopontin promotes pathologic mineralization in articular cartilage. *Matrix Biol.* **26,** 96–105
56. Weis, M. A., Hudson, D. M., Kim, L., Scott, M., Wu, J. J., and Eyre, D. R. (2010) Location of 3-hydroxyproline residues in collagen types I, II, III, and V/XI implies a role in fibril supramolecular assembly. *J. Biol. Chem.* **285,** 2580–2590
57. Vranka, J. A., Pokidysheva, E., Hayashi, L., Zientek, K., Mizuno, K., Ishikawa, Y., Maddox, K., Tufa, S., Keene, D. R., Klein, R., and Bächinger, H. P. (2010) Prolyl 3-hydroxylase 1 null mice display abnormalities in fibrillar collagen-rich tissues such as tendons, skin, and bones. *J. Biol. Chem.* **285,** 17253–17262
58. Marini, J. C., Cabral, W. A., and Barnes, A. M. (2010) Null mutations in LEPRE1 and CRTAP cause severe recessive osteogenesis imperfecta. *Cell Tissue Res.* **339,** 59–70
59. Christiansen, H. E., Schwarze, U., Pyott, S. M., AlSwaid, A., Al Balwi, M., Alrasheed, S., Pepin, M. G., Weis, M. A., Eyre, D. R., and Byers, P. H. (2010) Homozygosity for a missense mutation in SERPINH1, which encodes the collagen chaperone protein HSP47, results in severe recessive osteogenesis imperfecta. *Am. J. Hum. Genet.* **86,** 389–398
60. Cotterill, S. L., Jackson, G. C., Leighton, M. P., Wagener, R., Mäkitie, O., Cole, W. G., and Briggs, M. D. (2005) Multiple epiphyseal dysplasia mutations in MATN3 cause misfolding of the A-domain and prevent secretion of mutant matrilin-3. *Hum. Mutat.* **26,** 557–565
61. Vranka, J., Mokashi, A., Keene, D. R., Tufa, S., Corson, G., Sussman, M., Horton, W. A., Maddox, K., Sakai, L., and Bächinger, H. P. (2001) Selective intracellular retention of extracellular matrix proteins and chaperones associated with pseudoachondroplasia. *Matrix Biol.* **20,** 439–450
62. Hecht, J. T., Hayes, E., Haynes, R., and Cole, W. G. (2005) COMP mutations, chondrocyte function and cartilage matrix. *Matrix Biol.* **23,** 525–533
63. Leighton, M. P., Nundlall, S., Starborg, T., Meadows, R. S., Suleman, F., Knowles, L., Wagener, R., Thornton, D. J., Kadler, K. E., Boot-Handford, R. P., and Briggs, M. D. (2007) Decreased chondrocyte proliferation and dysregulated apoptosis in the cartilage growth plate are key features of a murine model of epiphyseal dysplasia caused by a matn3 mutation. *Hum. Mol. Genet.* **16,** 1728–1741
64. Nundlall, S., Rajpar, M. H., Bell, P. A., Clowes, C., Zeeff, L. A., Gardner, B., Thornton, D. J., Boot-Handford, R. P., and Briggs, M. D. (2010) An unfolded protein response is the initial cellular response to the expression of mutant matrilin-3 in a mouse model of multiple epiphyseal dysplasia. *Cell Stress Chaperones* **15,** 835–849
65. Piróg-Garcia, K. A., Meadows, R. S., Knowles, L., Heinegård, D., Thornton, D. J., Kadler, K. E., Boot-Handford, R. P., and Briggs, M. D. (2007) Reduced cell proliferation and increased apoptosis are significant pathological mechanisms in a murine model of mild pseudoachondroplasia resulting from a mutation in the C-terminal domain of COMP. *Hum. Mol. Genet.* **16,** 2072–2088
66. Rajpar, M. H., McDermott, B., Kung, L., Eardley, R., Knowles, L., Heeran, M., Thornton, D. J., Wilson, R., Bateman, J. F., Poulsom, R., Arvan, P., Kadler, K. E., Briggs, M. D., and Boot-Handford, R. P. (2009) Targeted induction of endoplasmic reticulum stress induces cartilage pathology. *PLoS Genet.* **5,** e1000691
67. Tsang, K. Y., Chan, D., Cheslett, D., Chan, W. C., So, C. L., Melhado, I. G., Chan, T. W., Kwan, K. M., Hunziker, E. B., Yamada, Y., Bateman, J. F., Cheung, K. M., and Cheah, K. S. (2007) Surviving endoplasmic reticulum stress is coupled to altered chondrocyte differentiation and function. *PLoS Biol.* **5,** e44
68. Honoré, B. (2009) The rapidly expanding CREC protein family: Members, localization, function, and role in disease. *Bioessays* **31,** 262–277
69. Iannotti, J. P., and Brighton, C. T. (1989) Cytosolic ionized calcium concentration in isolated chondrocytes from each zone of the growth plate. *J. Orthop. Res.* **7,** 511–518